Archives of Biochemistry and Biophysics 759 (2024) 110099

Contents lists available at ScienceDirect

Archives of Biochemistry and Biophysics

journal homepage: www.elsevier.com/locate/yabbi

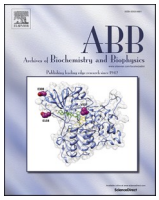

Dynamics of small molecule-enzyme interactions: Novel benzenesulfonamides as multi-target agents endowed with inhibitory effects against some metabolic enzymes

Özcan Güleç [a], Cüneyt Türkeş [b,**], Mustafa Arslan [a,*], Mesut Işık [c], Yeliz Demir [d], Hatice Esra Duran [e], Muhammet Fırat [f], Ömer İrfan Küfrevioğlu [g], Şükrü Beydemir [h]

[a] Department of Chemistry, Faculty of Arts and Science, Sakarya University, Sakarya, 54187, Turkey
[b] Department of Biochemistry, Faculty of Pharmacy, Erzincan Binali Yıldırım University, Erzincan, 24002, Turkey
[c] Department of Bioengineering, Faculty of Engineering, Bilecik Şeyh Edebali University, Bilecik, 11230, Turkey
[d] Department of Pharmacy Services, Nihat Delibalta Göle Vocational High School, Ardahan University, Ardahan, 75700, Turkey
[e] Department of Medical Biochemistry, Faculty of Medicine, Kafkas University, Kars, 36100, Turkey
[f] Department of Biotechnology, Graduate Institute, Bilecik Şeyh Edebali University, Bilecik, 11230, Turkey
[g] Department of Chemistry, Faculty of Sciences, Atatürk University, 25240, Erzurum, Turkey
[h] Department of Biochemistry, Faculty of Pharmacy, Anadolu University, Eskişehir, 26470, Turkey

ARTICLE INFO

Keywords:
Carbonic anhydrase
α-glycosidase
α-amylase
Sulfonamide
Tirazole
Oxadiazole
Molecular docking

ABSTRACT

In contemporary medicinal chemistry, employing a singular small molecule to concurrently multi-target disparate molecular entities is emerging as a potent strategy in the ongoing battle against metabolic disease. In this study, we present the meticulous design, synthesis, and comprehensive biological evaluation of a novel series of 1,2,3-triazolylmethylthio-1,3,4-oxadiazolylbenzenesulfonamide derivatives (**8a-m**) as potential multi-target inhibitors against human carbonic anhydrase (EC.4.2.1.1, *h*CA I/II), α-glycosidase (EC.3.2.1.20, α-GLY), and α-amylase (EC.3.2.1.1, α-AMY). Each synthesized sulfonamide underwent rigorous assessment for inhibitory effects against four distinct enzymes, revealing varying degrees of *h*CA I/II, a-GLY, and a-AMY inhibition across the tested compounds. *h*CA I was notably susceptible to inhibition by all compounds, demonstrating remarkably low inhibition constants (K_I) ranging from 42.20 ± 3.90 nM to 217.90 ± 11.81 nM compared to the reference standard AAZ (K_I of 439.17 ± 9.30 nM). The evaluation against *h*CA II showed that most of the synthesized compounds exhibited potent inhibition effects with K_I values spanning the nanomolar range 16.44 ± 1.53–70.82 ± 4.51 nM, while three specific compounds, namely **8a-b** and **8d**, showcased lower inhibitory potency than other derivatives that did not exceed that of the reference drug AAZ (with a K_I of 98.28 ± 1.69 nM). Moreover, across the spectrum of synthesized compounds, potent inhibition profiles were observed against diabetes mellitus-associated α-GLY (K_I values spanning from 0.54 ± 0.06 μM to 5.48 ± 0.50 μM), while significant inhibition effects were noted against α-AMY, with IC_{50} values ranging between 0.16 ± 0.04 μM and 7.81 ± 0.51 μM) compared to reference standard ACR (K_I of 23.53 ± 2.72 μM and IC_{50} of 48.17 ± 2.34 μM, respectively). Subsequently, these inhibitors were evaluated for their DPPH· and $ABTS^{+}$· radical scavenging activity. Moreover, molecular docking investigations were meticulously conducted within the active sites of *h*CA I/II, α-GLY, and α-AMY to provide comprehensive elucidation and rationale for the observed inhibitory outcomes.

Abbreviations: AAZ, acetazolamide; ACR, acarbose; ADME, absorption, distribution, metabolism, and excretion; AIC, akaike information criterion; α-GLY, α-glycosidase; α-AMY, α-amylase; BHT, hydroxytoluene; CA, carbonic anhydrase; K_I, inhibition constant; OPLS4, optimal potential liquid simulations 4; PDB, protein data bank; RMSD, root-mean-square deviation; TRX, trolox; XP, extra precision.

* Corresponding author. Department of Chemistry, Faculty of Arts and Sciences, Sakarya University, Sakarya, 54187, Turkey.
** Corresponding author. Department of Biochemistry, Faculty of Pharmacy, Erzincan Binali Yıldırım University, Erzincan, 24002, Turkey.
E-mail addresses: cuneyt.turkes@erzincan.edu.tr (C. Türkeş), marslan@sakarya.edu.tr (M. Arslan).

https://doi.org/10.1016/j.abb.2024.110099
Received 6 June 2024; Received in revised form 30 June 2024; Accepted 12 July 2024
Available online 14 July 2024

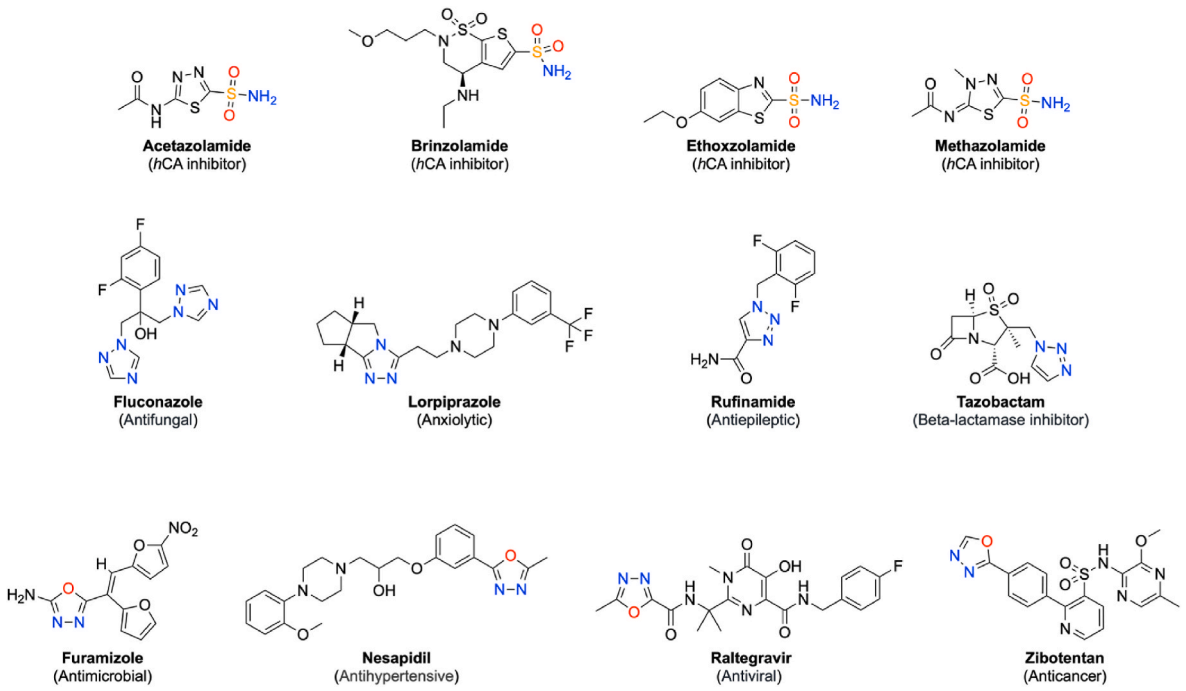

Fig. 1. Some bioactive molecules with sulfonamide, triazole, and oxadiazole core.

1. Introduction

In recent years, multi-target drugs have gained prominence as potential therapeutic options for diseases with complex origins and those associated with drug resistance [1,2]. While traditional single-target treatments are designed to minimize off-target effects, they often fail to address the multifaceted nature of many diseases fully [3]. Complex disorders typically arise from the interaction of various genetic and environmental factors, leading to robust pathological conditions [4]. Therefore, simultaneous modulation of multiple targets appears more promising for effectively managing such situations [5].

Sulfonamides represent a consequential subset within the category of sulfa drugs [6], emerging as prominent pharmacophores under their distinctive attributes, encompassing diminished toxicity [7], oral bioavailability [8], cost-effectiveness [9], and heightened reactivity [10]. Given their multifaceted biological effects, spanning antibacterial [11], anti-inflammatory [12], antiviral [13], anti-diabetic [14], and carbonic anhydrase (CA, EC.4.2.1.1) inhibitory properties [15], sulfonamide derivatives have proliferated extensively, with thousands synthesized and employed extensively in the therapeutic management of diverse pathological conditions. Furthermore, in recent decades, there has been a notable surge in the synthesis of novel 1,3,4-oxadiazole and 1,2,3-triazole derivatives and the subsequent investigation into their biological activities [16]. These compounds have emerged as pivotal building blocks in the development of a diverse array of pharmaceutical agents [17,18], exhibiting multifaceted therapeutic potentials encompassing antibacterial [19,20], antifungal [21,22], analgesic [23,24], anti-inflammatory [25,26], antiviral [27,28], anticancer [29,30], antihypertensive [31], anticonvulsant [32,33], anti-diabetic properties [34,35], and some metabolic enzyme inhibitors, such as CA [36], α-glycosidase (α-GLY, EC.3.2.1.20) [37,38], and α-amylase (α-AMY, EC.3.2.1.1) [39,40] (Fig. 1).

The CAs represent a ubiquitous class of metalloenzymes with paramount significance in biological systems [41], orchestrating the reversible conversion of carbon dioxide (CO_2) into hydrogen carbonate ions (HCO^{3-}) and protons (H^+) [42], thereby modulating crucial water-soluble products pivotal for pH homeostasis [43]. The human proteome currently delineates 16 distinct CA isoforms [44], each intricately woven into a complex tapestry of physiological and biochemical cascades, including but not limited to pH regulation [45], gluconeogenesis [46], secretory processes [47], and oncogenic pathways [48]. At the molecular level, the catalytic prowess of human carbonic anhydrases (*h*CAs) is encapsulated within their active sites, characterized by a tetrahedral coordination geometry orchestrated by zinc ions [49], which are intricately bound by a triumvirate of amino acid residues (namely, His94, His96, and His119) [50] in conjunction with a water molecule or hydroxide ion [51]. Among these isoforms, cytosolic *h*CA I occupy a secondary role, whereas cytosolic *h*CA II emerges as a preeminent therapeutic target [52], particularly in managing glaucoma due to its indispensable role in regulating intraocular pressure [53]. Achieving selective inhibition of *h*CA II while mitigating off-target effects remains an ongoing pursuit. Conventionally, the inhibition of CAs necessitates the incorporation of zinc-binding functionalities [54], with benzenesulfonamide motifs being favored for their ability to coordinate the metal ion in either tetrahedral or bipyramidal configurations [55]. The endeavor to tailor selective *h*CA inhibitors (*h*CAIs) involves the strategic retention of the sulfonamide group while effecting structural modifications within the core scaffold of the molecule, leveraging a nuanced "tail approach" [56,57]. This intricate design strategy facilitates the customization of tail functionalities appended to the heterocyclic/aromatic moiety, thereby affording optimal interactions with both the conserved central residues and the variably exposed peripheral regions of the active site, which exhibit notable divergence across distinct *h*CA isoforms [58].

Noninsulin-dependent diabetes mellitus, a prevalent disorder of the endocrine system, manifests as a consequence of diminished insulin secretion by pancreatic Langerhans β cells or heightened insulin resistance stemming from excessive glucose absorption [59]. The management of diabetes encompasses a diverse array of pharmacological interventions, each exerting distinct modes of action, including but not limited to insulin secretion stimulation, augmentation of glucose transporter expression, gluconeogenesis inhibition, and attenuation of intestinal glucose absorption [60]. Given the multifaceted nature of diabetes and its propensity for precipitating numerous complications, a multifaceted therapeutic approach is imperative [61]. Particularly in the prediabetic phase characterized by insulin resistance, glycemic control

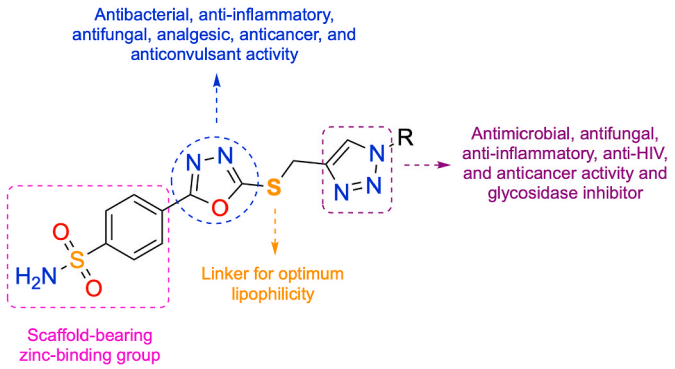

Fig. 2. The design strategy of targeted 1,2,3-triazolylmethylthio-1,3,4-oxadiazolylbenzenesulfonamides (**8a-m**).

can be effectively achieved through the administration of oral agents targeting glucose absorption, such as α-GLY and/or pancreatic α-AMY inhibitors [62].

Within the framework of our research design, we sought to elucidate the impact of novel multi-target molecular hybrid compounds on the inhibition of some metabolic enzymes. Consequently, the structural design of these compounds was predicated upon incorporating the 1,3,4-oxadiazole ring as a central scaffold, wherein a benzenesulfonamide moiety was strategically introduced as a zinc-binding group at the 2 position. Concurrently, the 5 position of the scaffold was substituted with a 1,2,3-triazolylmethylthio moiety, accommodating various electron-withdrawing and/or -donating functional groups (Fig. 2).

Building upon the aforementioned rationale, we present herein the detailed design and synthesis of a novel series of 1,2,3-triazolylmethylthio-1,3,4-oxadiazolylbenzenesulfonamide derivatives (**8a-m**) as potential multi-target inhibitors of *h*CAs, α-GLY, and α-AMY (Scheme 1). These molecules represent a novel class of compounds and within the scope of our current research endeavor, we provide a comprehensive account of the synthetic methodologies employed for preparing a library of small molecules based on the aforementioned scaffolds. Subsequently, we report the synthesized compounds underwent a rigorous evaluation to ascertain their *in vitro* and *in silico* efficacy against *h*CA I and II isoforms, α-GLY, and α-AMY.

2. Materials and methods

2.1. Chemistry

Melting points were determined by a Yanagimoto micro-melting point apparatus and were uncorrected. IR spectra were acquired on a SHIMADZU Prestige-21 (200 VCE) spectrometer. ^{1}H and ^{13}C NMR spectra were acquired at VARIAN Infinity Plus at 300 and 75 Hz, respectively. ^{1}H and ^{13}C chemical shifts are referenced to the internal deuterated solvent. The Mass analysis was carried out with an LC/MS QTOF-9030 spectroscopy. All chemicals were purchased from Merck, Alfa Aesar, and Sigma-Aldrich.

2.2. General procedure for preparation of 4-sulfonylamide ester (2)

Sulfamoylbenzoic acid (10 mmol) and 1.0 ml sulfuric acid were refluxed for 24 h in 50 ml of ethanol. At the reaction's end, the solvent evaporated, and the obtained product was washed and dried in cold water. The purity of the compound was checked by ^{1}H and ^{13}C NMR. The compound was used for the next step without further purification.

2.3. General procedure for preparation of 4-sulfonylamidebenzohydrazide (3)

4-sulfonylamide ester (10 mmol) and Hydrazine hydrate (25 mmol) in ethanol were refluxed for 24 h at 70 °C. At the end of the reaction, the reaction mixture was cooled to room temperature, and the solid was filtered, then washed with water and dried. The purity of the compound was checked by ^{1}H and ^{13}C NMR. The compound was used for the next

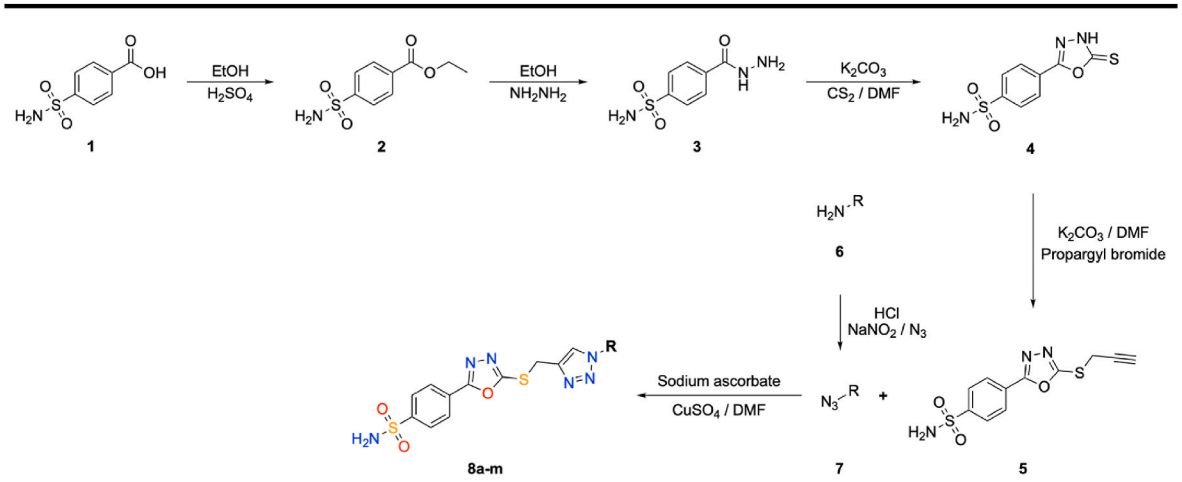

Compound					
ID	**R**	**ID**	**R**	**ID**	**R**
8a	Pentyl	**8f**	4-Chlorophenyl	**8j**	4-Cyanophenyl
8b	Phenyl	**8g**	2-Chlorophenyl	**8k**	5-Chloro-2-nitrophenyl
8c	4-Hydroxyphenyl	**8h**	4-Fluorophenyl	**8l**	4-Sulfamoylphenyl
8d	4-Iodophenyl	**8i**	3-Fluorophenyl	**8m**	4-Carboxyphenyl
8e	4-Bromophenyl				

Scheme 1. Synthetic pathway of targeted novel 1,2,3-triazolylmethylthio-1,3,4-oxadiazolylbenzenesulfonamides (**8a-m**).

step without further purification.

2.4. General procedure for the synthesis of 4-(5-thioxo-4,5-dihydro-1,3,4-oxadiazol-2-yl)benzenesulfonamide (4)

Carbon disulphur (2.5 mmol) and 4-sulfonylamidebenzohydrazide (1 mmol) were dissolved in DMF (6 ml), and K_2CO_3 (2 mmol) was added to the mixture. Then, the mixture was stirred for 12 h at room temperature. After the reaction was completed, the mixture was poured into ice-cold water. It was then filtered and crystallized from acetone. The purity of the compound was checked by ^1H and ^{13}C NMR. The compound was used for the next step without further purification.

2.5. General procedure for the synthesis of 4-[5-(prop-2-yn-1-ylthio)-1,3,4-oxadiazol-2-yl]benzenesulfonamide (5)

Propargyl bromide (1 mmol) and 4-(5-thioxo-4,5-dihydro-1,3,4-oxadiazol-2-yl)benzenesulfonamide (1 mmol) were dissolved in DMF (6 ml) and K_2CO_3 (2 mmol) was added to the mixture. Then, the mixture was stirred for 12 h at room temperature. After the reaction was completed, the mixture was poured into ice-cold water. It was then filtered and crystallized through acetone. The purity of the compound was checked by ^1H and ^{13}C NMR. The compound was used for the next step without further purification.

2.6. General procedure for the synthesis of azidobenzene derivatives (7)

Aniline derivatives (3 mmol) were added to 15 ml of water. 5 ml of 37 % HCl was added to it. After aniline derivatives were dissolved, the mixture was cooled to 0 °C with an ice bath. Sodium nitrite (4 mmol) was slowly added to the mixture by dissolving in 15 ml water at 0 °C. It was allowed to mix for one more hour at the same temperature. Then, sodium azide (4 mmol) was added slowly at 0 °C and stirred for 12 h at room temperature. After the reaction was completed. The reaction mixture was extracted with ethylacetate. The purity of the compound was checked by ^1H and ^{13}C NMR. The compound was used for the next step without further purification.

2.7. General procedure for the synthesis of aromatic trazole substituted 4-(5-thioxo-4,5-dihydro-1,3,4-oxadiazol-2-yl)benzenesulfonamide derivatives (8a-m)

Azidobenzene derivatives (1 mmol) and 4-[5-(prop-2-yn-1-ylthio)-1,3,4-oxadiazol-2-yl]benzenesulfonamide (1 mmol) were dissolved in DMF (6 ml), and then $CuSO_4$ (0,1 mmol) and Sodium ascorbate (0,1 mmol) was added to the mixture. The mixture was stirred for 12 h at room temperature. After the reaction was completed. The mixture was poured into ice-cold water. It was then filtered and crystallized from acetone. The prepared compounds shown in Scheme 1 were characterized by ^1H NMR, ^{13}C NMR, FT-IR, and LC/MS QTOF-9030 spectroscopy.

2.7.1. 4-[5-{[(1-Pentyl-1H-1,2,3-triazol-4-yl)methyl]thio}-1,3,4-oxadiazol-2-yl]benzenesulfonamide (8a)

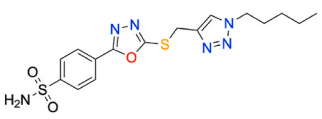

Yield: 85 %; M.p. 157–158 °C; FT-IR (ν, cm^{-1}): 3336 (NH_2), 2955 (C═C–H), 1472 (C═N), 1340, 1156 (SO_2); ^1H NMR (300 MHz, DMSO-d_6, ppm): δ 8.17 (d, J = 9.0 Hz, 2H, =CH), 8.14 (s, 1H, triazole ring C–H), 8.01 (d, J = 8.1 Hz, 2H, =CH), 7.60 (s, 2H, –NH_2), 4.67 (s, 2H, –SCH_2), 4.32 (t, J = 7.1 Hz, 2H, –CH_2), 1.82–1.68 (m, 2H, –CH_2), 1.35–1,05 (m, 4H, –CH_2), 0.79 (t, J = 7.0 Hz, 3H, –CH_3). ^{13}C NMR (75 MHz, DMSO-d_6, ppm): δ 165.05 and 164.65 (oxadiazole ring), 147.45, 147.35, 127.65, 127.63, 127.39, 126.46, 50.17, 30.15, 28.68, 27.56 (SCH_2); QTOF LC-MS (m/z) found: $[M+H]^+$; 409.1040, calcd. for $[C_{16}H_{20}N_6O_3S_2]$; 408.1038 $[M]^+$.

2.7.2. 4-[5-{[(1-Phenyl-1H-1,2,3-triazol-4-yl)methyl]thio}-1,3,4-oxadiazol-2-yl]benzenesulfonamide (8b)

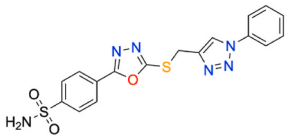

Yield: 92 %; M.p. 219–221 °C; FT-IR (ν, cm^{-1}): 3320 (NH_2), 2951 (C═C–H), 1462 (C═N), 1342, 1167 (SO_2); ^1H NMR (300 MHz, DMSO-d_6, ppm): δ 8.81 (s, 1H, triazole ring C–H), 8.16 (d, J = 8.1 Hz, 2H, =CH), 7.98 (d, J = 8.1 Hz, 2H, =CH), 7.86 (d, J = 8.3 Hz, 2H, =CH), 7.57 (t, J = 7.7 Hz, 2H, =CH), 7.54 (s, 2H, –NH_2), 7.47 (t, J = 7.0 Hz, 1H, =CH), 4.75 (s, 2H, –SCH_2); ^{13}C NMR (75 MHz, DMSO-d_6, ppm): δ 165.19 and 164.45 (oxadiazole ring), 147.38, 144.27, 137.11, 130.60, 130.45, 129.49, 127.80, 126.51, 122.84, 120.78, 27.44 (SCH_2); QTOF LC-MS (m/z) found: $[M+H]^+$; 415.0572, calcd. for $[C_{17}H_{14}N_6O_3S_2]$; 414.0569 $[M]^+$.

2.7.3. 4-[5-({[1-(4-Hydroxyphenyl)-1H-1,2,3-triazol-4-yl]methyl}thio)-1,3,4-oxadiazol-2-yl]benzenesulfonamide (8c)

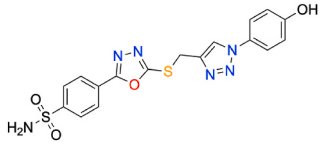

Yield: 80 %; M.p. 134–135 °C; FT-IR (ν, cm^{-1}): 3499 (OH), 3309 (NH_2), 2958 (C═C–H), 1474 (C═N), 1329, 1169 (SO_2); ^1H NMR (300 MHz, DMSO-d_6, ppm): δ 9.97 (s, 1H, –OH), 8.63 (s, 1H, triazole ring C–H), 8.16 (d, J = 8.1 Hz, 2H, =CH), 7.99 (d, J = 8.2 Hz, 2H, =CH), 7.63 (d, J = 7.5 Hz, 2H, =CH), 7.59 (s, 2H, –NH_2), 6.90 (d, J = 8.4 Hz, 2H, =CH), 4.73 (s, 2H, –SCH_2); ^{13}C NMR (75 MHz, DMSO-d_6, ppm): δ 165.16 and 164.49 (oxadiazole ring), 158.48, 147.34, 129.25, 127.81, 127.37, 126.51, 122.71, 122.66, 116.71, 116.62, 27.45 (SCH_2); QTOF LC-MS (m/z) found: $[M+H]^+$; 431.0519, calcd. for $[C_{17}H_{14}N_6O_4S_2]$; 430.0518 $[M]^+$.

2.7.4. 4-[5-({[1-(4-Iodophenyl)-1H-1,2,3-triazol-4-yl]methyl}thio)-1,3,4-oxadiazol-2-yl]benzenesulfonamide (8d)

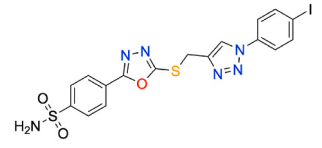

Yield: 87 %; M.p. 235–237 °C; FT-IR (ν, cm^{-1}): 3245 (NH_2), 2987 (C═C–H), 1467 (C═N), 1340, 1155 (SO_2); ^1H NMR (300 MHz, DMSO-d_6, ppm): δ 8.83 (s, 1H, triazole ring C–H), 8.16 (d, J = 8.1 Hz, 2H, =CH), 7.99 (d, J = 8.2 Hz, 2H, =CH), 7.93 (d, J = 8.3 Hz, 2H, =CH), 7.69 (d, J = 8.3 Hz, 2H, =CH), 7.59 (s, 2H, –NH_2), 4.75 (s, 2H, –SCH_2); ^{13}C NMR (75 MHz, DMSO-d_6, ppm): δ 165.17 and 164.43 (oxadiazole ring), 147.36, 139.26, 139.19, 136.76, 127.80, 127.38, 126.50, 122.76, 122.62, 95.18, 27.37(SCH_2); QTOF LC-MS (m/z) found: $[M+H]^+$; 540.9539, calcd. for $[C_{17}H_{13}IN_6O_3S_2]$; 539.9535 $[M]^+$.

*2.7.5. 4-[5-({[1-(4-Bromophenyl)-1H-1,2,3-triazol-4-yl]methyl}thio)-1,3,4-oxadiazol-2-yl]benzenesulfonamide (**8e**)*

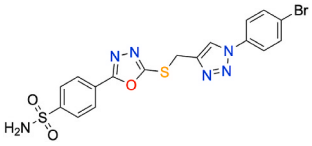

Yield: 82 %; M.p. 241–243 °C; FT-IR (ν, cm^{-1}): 3332 (NH_2), 2958 (C═C–H), 1464 (C═N), 1332, 1162 (SO_2); ^1H NMR (300 MHz, DMSO-d_6, ppm): δ 8.85 (s, 1H, triazole ring C–H), 8.16 (d, J = 6.2 Hz, 2H, =CH), 8.00 (d, J = 8.3 Hz, 2H, =CH), 7.85 (d, J = 6.5 Hz, 2H, =CH), 7.77 (d, J = 8.9 Hz, 2H, =CH), 7.58 (s, 2H, –NH_2), 4.76 (s, 2H, –SCH_2);^{13}C NMR (75 MHz, DMSO-d_6, ppm): δ 165.19 and 164.41(oxadiazole ring), 147.40, 144.32, 136.34, 133.48, 127.81, 127.38, 126.50, 122.90, 122.72, 122.14, 27.36(SCH_2); QTOF LC-MS (m/z) found: $[M+H]^+$; 494.4593, calcd. for $[C_{17}H_{13}BrN_6O_3S_2]$; 493.4590 $[M]^+$.

*2.7.6. 4-[5-({[1-(4-Chlorophenyl)-1H-1,2,3-triazol-4-yl]methyl}thio)-1,3,4-oxadiazol-2-yl]benzenesulfonamide (**8f**)*

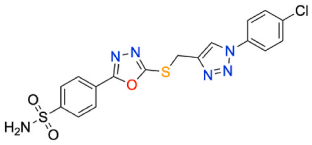

Yield: 93 %; M.p. 228–231 °C; FT-IR (ν, cm^{-1}): 3334 (NH_2), 2971 (C═C–H), 1464 (C═N), 1339, 1163 (SO_2); ^1H NMR (300 MHz, DMSO-d_6, ppm): δ 8.87 (s, 1H, triazole ring C–H), 8.18 (d, J = 8.7 Hz, 2H, =CH), 8.01 (d, J = 8.1 Hz, 2H, =CH), 7.93 (d, J = 8.2 Hz, 2H, =CH), 7.67 (d, J = 8.9 Hz, 2H, =CH), 7.61 (s, 2H, –NH_2), 4.78 (s, 2H, –SCH_2); ^{13}C NMR (75 MHz, DMSO-d_6, ppm): δ 165.18 and 164.42(oxadiazole ring), 147.38, 135.92, 133.73, 130.56, 127.81, 127.38, 126.50, 123.03, 123.02, 122.47, 27.34(SCH_2); QTOF LC-MS (m/z) found: $[M+H]^+$; 449.0182, calcd. for $[C_{17}H_{13}BrN_6O_3S_2]$; 448.0179 $[M]^+$.

*2.7.7. 4-[5-({[1-(2-Chlorophenyl)-1H-1,2,3-triazol-4-yl]methyl}thio)-1,3,4-oxadiazol-2-yl]benzenesulfonamide (**8g**)*

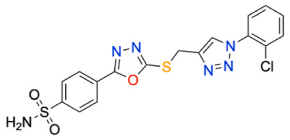

Yield: 86 %; M.p. 186–187 °C; FT-IR (ν, cm^{-1}): 3355 (NH_2), 2958 (C═C–H), 1470 (C═N), 1326, 1152 (SO_2); ^1H NMR (300 MHz, DMSO-d_6, ppm): δ 8.56 (s, 1H, triazole ring C–H), 8.16 (d, J = 8.2 Hz, 2H, =CH), 7.99 (d, J = 8.3 Hz, 2H, =CH), 7.73 (d, J = 6.2 Hz, 1H, =CH), 7.65 (t, J = 7.4 Hz, 1H, =CH), 7.61 (m,1H, =CH), 7.58 (s, 2H, –NH_2), 7.54 (d, J = 7.8 Hz, 1H, =CH), 4.77 (s, 2H, –SCH_2); ^{13}C NMR (75 MHz, DMSO-d_6, ppm): δ 165.22 and 164.41(oxadiazole ring), 147.40, 134.99, 132.40, 131.22, 129.17, 129.07, 128.99, 127.82, 127.82, 127.37, 126.80, 126.48, 27.41(SCH_2); QTOF LC-MS (m/z) found: $[M+H]^+$; 449.0183, calcd. for $[C_{17}H_{13}ClN_6O_3S_2]$; 448,0179 $[M]^+$.

*2.7.8. 4-[5-({[1-(4-Fluorophenyl)-1H-1,2,3-triazol-4-yl]methyl}thio)-1,3,4-oxadiazol-2-yl]benzenesulfonamide (**8h**)*

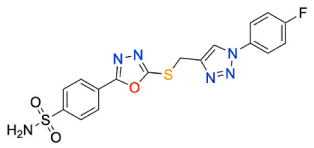

Yield: 75 %; M.p. 232–233 °C; FT-IR (ν, cm^{-1}): 3327 (NH_2), 2987 (C═C–H), 1464 (C═N), 1350, 1167 (SO_2); ^1H NMR (300 MHz, DMSO-d_6, ppm): δ 8.80 (s, 1H, triazole ring C–H), 8.16 (d, J = 8.5 Hz, 2H, =CH), 7.98 (d, J = 8.4 Hz, 2H, =CH), 7.95–7.87 (m, 2H, =CH), 7.59 (s, 2H, –NH_2), 7.43 (t, J = 9.0 Hz, 2H, =CH), 4.75 (s, 2H, –SCH_2); ^{13}C NMR (75 MHz, DMSO-d_6, ppm): δ 163.23 and 155.20(oxadiazole ring), 147.62, 132.20, 129.66, 129.55, 127.85, 127.06, 126.91, 116.46, 116.17, 92.66, 42.21(SCH_2); QTOF LC-MS (m/z) found: $[M+H]^+$; 433.0478, calcd. for $[C_{17}H_{13}FN_6O_3S_2]$; 432.0475 $[M]^+$.

*2.7.9. 4-[5-({[1-(3-Fluorophenyl)-1H-1,2,3-triazol-4-yl]methyl}thio)-1,3,4-oxadiazol-2-yl]benzenesulfonamide (**8i**)*

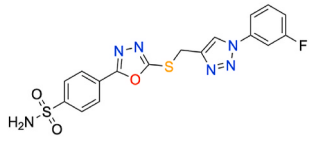

Yield: 84 %; M.p. 206–208 °C; FT-IR (ν, cm^{-1}): 3266 (NH_2), 2961 (C═C–H), 1463 (C═N), 1344, 1165 (SO_2); ^1H NMR (300 MHz, DMSO-d_6, ppm): δ 8.91 (s, 1H, triazole ring C–H), 8.18 (d, J = 6.5 Hz, 2H, =CH), 8.00 (d, J = 8.6 Hz, 2H, =CH), 7.90–7.73 (m, 2H, =CH), 7.67 (d, J = 8.4 Hz, 1H, =CH), 7.60 (s, 2H, –NH_2), 7.36 (t, J = 8.6 Hz, 1H, =CH), 4.78 (s, 2H, –SCH_2); ^{13}C NMR (75 MHz, DMSO-d_6, ppm): δ 165.19 and 164.43(oxadiazole ring), 161.43, 147.34, 138.22, 132.62, 132.50, 127.80, 127.37, 126.49, 123.03, 116.68, 116.07, 108.07, 27.31(SCH_2); QTOF LC-MS (m/z) found: $[M+H]^+$; 433.0477, calcd. for $[C_{17}H_{13}FN_6O_3S_2]$; 432,0475 $[M]^+$.

*2.7.10. 4-[5-({[1-(4-Cyanophenyl)-1H-1,2,3-triazol-4-yl]methyl}thio)-1,3,4-oxadiazol-2-yl]benzenesulfonamide (**8j**)*

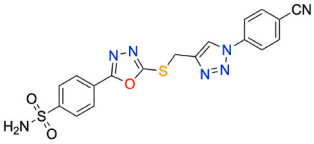

Yield: 80 %; M.p. 268–269 °C; FT-IR (ν, cm^{-1}): 3248 (NH_2), 3007 (C═C–H), 1466 (C═N), 1342, 1165 (SO_2); ^1H NMR (300 MHz, DMSO-d_6, ppm): δ 8.99 (s, 1H, triazole ring C–H), 8.18 (d, J = 8.6 Hz, 2H, =CH), 8.13 (d, J = 8.6 Hz, 2H, =CH), 8.09 (d, J = 8.9 Hz, 2H, =CH), 8.01 (d, J = 8.5 Hz, 2H, =CH), 7.60 (s, 2H, –NH_2), 4.79 (s, 2H, –SCH_2).^{13}C NMR (75 MHz, DMSO-d_6, ppm): δ 165.35 and 164.34(oxadiazole ring), 147.45, 144.76, 140.03, 134.98, 127.80, 127.37, 126.49, 123.10, 121.20, 118.77, 111.82(CN), 27.29(SCH_2); QTOF LC-MS (m/z) found: $[M+H]^+$; 440.0525, calcd. for $[C_{18}H_{14}N_7O_3S_2]$, 439.0521 $[M]^+$.

*2.7.11. 4-[5-({[1-(5-Chloro-2-nitrophenyl)-1H-1,2,3-triazol-4-yl]methyl}thio)-1,3,4-oxadiazol-2-yl]benzenesulfonamide (**8k**)*

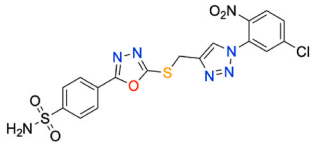

Yield: 88 %; M.p. 201–203 °C; FT-IR (ν, cm^{-1}): 3365 (NH_2), 3046 (C═C–H), 1527 (C═N), 1600, 1364 (NO_2), 1333, 1155 (SO_2); ^{1}H NMR (300 MHz, DMSO-d_6, ppm): δ 8.76 (s, 1H, triazole ring C–H), 8.25 (d, J = 8.8 Hz, 2H, =CH), 8.19 (d, J = 7.1 Hz, 2H, =CH), 8.12 (s, 1H, =CH), 8.01 (d, J = 8.0 Hz, 1H, =CH), 7.94 (d, J = 8.1 Hz, 1H, =CH), 7.61 (s, 2H, –NH_2), 4.81 (s, 2H, –SCH_2); ^{13}C NMR (75 MHz, DMSO-d_6, ppm): δ 165.21 and 164.38(oxadiazole ring), 147.39, 144.01, 143.28, 139.15, 131.74, 130.76, 128.28, 127.94, 127.82, 127.38, 126.49, 126.11, 27.21 (SCH_2); QTOF LC-MS (m/z) found: $[M+H]^+$; 494.0918, calcd. for $[C_{17}H_{12}ClN_7O_5S_2]$; 493.0915 $[M]^+$.

2.7.12. 4-[4-({[5-(4-Sulfamoylphenyl)-1,3,4-oxadiazol-2-yl]thio} methyl)-1H-1,2,3-triazol-1-yl]benzenesulfonamide (8l)

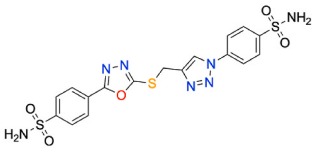

Yield: 92 %; M.p. 285–286 °C; FT-IR (ν, cm^{-1}): 3355 (NH_2), 3073 (C═C–H), 1463 (C═N), 1333, 1152 (SO_2); ^{1}H NMR (300 MHz, DMSO-d_6, ppm): δ 8.94 (s, 1H, triazole ring C–H), 8.19 (d, J = 8.5 Hz, 2H, =CH), 8.12 (d, J = 8.8 Hz, 2H, =CH), 8.01 (d, J = 7.2 Hz, 4H), 7.59 (s, 2H, –NH_2), 7.54 (s, 2H, –NH_2), 4.80 (s, 2H, –SCH_2); ^{13}C NMR (75 MHz, DMSO-d_6, ppm): δ 165.20 and 164.43(oxadiazole ring), 147.38, 144.57, 139.14, 128.28, 128.20, 127.81, 127.39, 126.52, 123.06, 121.07, 27.38(SCH_2); QTOF LC-MS (m/z) found: $[M+H]^+$; 494.0300, calcd. for $[C_{17}H_{16}N_7O_5S_3]$; 493.0297 $[M]^+$.

2.7.13. 4-[4-({[5-(4-Sulfamoylphenyl)-1,3,4-oxadiazol-2-yl]thio} methyl)-1H-1,2,3-triazol-1-yl]benzoic acid (8m)

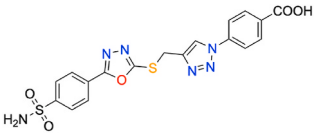

Yield: 85 %; M.p. 279–280 °C; FT-IR (ν, cm^{-1}): 2800–3500 (COOH), 3273 (NH_2), 2958 (C═C–H), 1691 (C═O), 1461 (C═N), 1334, 1158 (SO_2); ^{1}H NMR (300 MHz, DMSO-d_6, ppm): δ 8.95 (s, 1H, triazole ring C–H), 8.19 (d, J = 8.4 Hz, 2H, =CH), 8.14 (d, J = 8.3 Hz, 2H, =CH), 8.06 (d, J = 8.3 Hz, 2H, =CH), 8.02 (d, J = 8.1 Hz, 2H, =CH), 7.61 (s, 2H, –NH_2), 4.80 (s, 2H, –SCH_2); ^{13}C NMR (75 MHz, DMSO-d_6, ppm): δ 167.12(COOH), 165.20 and 164.41(oxadiazole ring), 147.38, 144.54, 139.97, 131.77, 131.59, 127.81, 127.38, 126.51, 122.96, 120.51, 27.35 (SCH_2); QTOF LC-MS (m/z) found: $[M+H]^+$; 459.0470, calcd. for $[C_{18}H_{14}N_6O_5S_2]$; 458.0467 $[M]^+$.

2.8. Biological study

2.8.1. Inhibitory effect study

The *h*CA isoforms I and II were purified from human erythrocytes using Sepharose-4B-L-tyrosine-sulfanilamide affinity chromatography, following the protocols established in our prior study [63]. The assessment of novel 1,2,3-triazolylmethylthio-1,3,4-oxadiazolylbenzenesulfonamide derivatives (**8a-m**) inhibition effects on the esterase activity of *h*CAs was conducted through meticulous monitoring of absorbance changes at 348 nm in accordance with the protocol delineated by Verpoorte et al. [64]. The enzymatic activities of *h*CAs were quantified utilizing 4-nitrophenyl acetate, consistent with prior methodologies. The α-GLY from *Saccharomyces cerevisiae* (G5003, CAS number: 9001-42-7) and α-AMY from porcine pancreas (A6255) were sourced from Sigma-Aldrich Chemie GmbH in Taufkirchen, Germany. The α-GLY activity was meticulously assessed utilizing para-nitrophenyl-α-D-glucopyranoside as the substrate, adhering closely to the experimental protocol outlined by Tao et al. [65]. Notably, in this context, one unit of α-GLY activity is defined as the quantity of enzyme catalyzing the hydrolysis of 1.0 mol of substrate per minute under standardized conditions at pH 7.4. The determination of α-AMY activity in this study adhered to the methodology documented by Xiao et al. [66]. Absorbance measurements were subsequently obtained spectrophotometrically at 580 nm. In this context, one unit of α-amylase enzyme activity is defined as the quantity of enzyme that liberates 1.0 mg of maltose from starch within 3 min under standardized conditions at pH 6.9 and 20 °C. Notably, rigorous experimental precision was ensured by triply replicating all measurements.

The inhibitory potency of newly synthesized derivatives was comprehensively investigated, employing no fewer than five distinct inhibitor concentrations for both *h*CAs, α-GLY, and α-AMY. IC_{50} values for these synthesized derivatives were determined from activity (%) graphs for each compound (designated as **8a-m**). Discrimination between inhibition types and the elucidation of inhibition constants was achieved by applying Lineweaver and Burk's plot analysis [67].

2.8.2. DPPH· and $ABTS^+$· radical scavenging activity study

The assessment of DPPH· and $ABTS^+$· free radical scavenging activity was conducted in accordance with the methodology outlined by Blois [68] and Re et al. [69], respectively. The novel 1,2,3-triazolylmethylthio-1,3,4-oxadiazolylbenzenesulfonamide derivatives (**8a-m**) under investigation, previously prepared at a concentration of 1 mg/ml, were employed in the assay. Initially, a solution of 1 mM DPPH· served as the source of free radicals. Test tubes were laden with aliquots of the sample stock solution to yield concentrations of 10, 20, and 30 μg/μl, with the total volume adjusted to 2 ml using ethanol. Subsequently, 0.5 ml of the DPPH· solution was introduced into each sample tube. After a 30-min incubation period in a light-protected environment at ambient temperature, absorbance readings were recorded at 517 nm. Later, a 7 mM solution of $ABTS^+$· was prepared, and $ABTS^+$· radicals were generated by adding a 2.45 mM persulfate solution. The absorbance of a control solution at 734 nm was adjusted to 0.700 ± 0.025 nm before utilizing the $ABTS^+$· radical solution. Various concentrations (10, 20, and 30 μg/ml) of ethyl alcohol extracts derived from the solutions were subjected to the assay, where 0.5 ml of the $ABTS^+$· radical solution was added to each concentration. Following a 30-min incubation, absorbance measurements were conducted at 734 nm against a blank containing ethanol.

2.9. In silico study

In this study, molecular docking analysis was conducted utilizing the latest iteration of the Small-Molecule Drug Discovery Suite tailored for Macintosh, denoted as version 2024-1. The protein data bank (PDB) IDs, namely 1AZM [70], 3HS4 [71], and 5NN8 [72], were procured from the RCSB Protein Data Bank and served as the foundational models for the experimental procedures, representing *h*CA I and II isoforms, as well as α-GLY, respectively. These structural representations underwent meticulous preparation for docking by applying the Protein Preparation Wizard [73] within the Small-Molecule Drug Discovery Suite [74]. The molecular structures of novel 1,2,3-triazolylmethylthio-1,3,4-oxadiazolylbenzenesulfonamide derivatives (**8a-m**) were meticulously crafted using the ChemDraw program, version 21 (PerkinElmer, Inc., Waltham, MA, USA) tailored for Macintosh. Subsequently, these structures were subjected to optimization employing the LigPrep module [75,76] within the same software suite, utilizing the optimal potential liquid simulations 4 (OPLS4) force field with Epik [77] under pH 7.4 ± 0.5 conditions [78]. The identification of active site residues, crucial for docking, was facilitated through the SiteMap tool [79] and further utilized in the Receptor Grid Generation module [80] to construct the receptor grid within the Maestro panel [81,82]. Docking of ligands to *h*CAs and α-GLY

Table 1
Inhibitory effects of the novel 1,2,3-triazolylmethylthio-1,3,4-oxadiazolylbenzenesulfonamides (**8a-m**) on *h*CA I, II isoforms, α-GLY, and α-AMY.

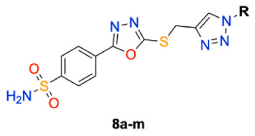

8a-m

Compound		*h*CA I[a]		*h*CA II[b]		α-GLY[c]		α-AMY[d]	
ID	R	K_I[e] (nM)	R^2	K_I[e] (nM)	R^2	K_I[e] (μM)	R^2	IC_{50}[e] (μM)	R^2
8a	Pentyl	81.42 ± 7.37	0.9888	158.20 ± 9.73	0.9877	0.54 ± 0.06	0.9880	7.81 ± 0.51	0.9849
8b	Phenyl	217.90 ± 11.81	0.9885	253.70 ± 17.70	0.9879	ND[h]	ND[h]	1.15 ± 0.16	0.9933
8c	4OH-Ph	212.30 ± 13.85	0.9863	42.81 ± 3.83	0.9888	1.67 ± 0.11	0.9862	0.72 ± 0.11	0.9960
8d	4I-Ph	69.41 ± 6.85	0.9883	165.40 ± 10.85	0.9894	1.06 ± 0.10	0.9879	1.03 ± 0.08	0.9979
8e	4Br-Ph	156.60 ± 9.51	0.9889	24.36 ± 2.10	0.9893	1.52 ± 0.15	0.9867	0.85 ± 0.21	0.9807
8f	4Cl-Ph	56.01 ± 5.75	0.9875	16.44 ± 1.53	0.9883	1.05 ± 0.07	0.9880	0.88 ± 0.10	0.9950
8g	2Cl-Ph	58.48 ± 3.39	0.9888	57.79 ± 4.03	0.9863	0.98 ± 0.10	0.9866	0.16 ± 0.04	0.9988
8h	4F-Ph	43.94 ± 4.45	0.9875	70.82 ± 4.51	0.9873	0.61 ± 0.06	0.9890	0.55 ± 0.07	0.9985
8i	3F-Ph	66.16 ± 6.84	0.9868	55.11 ± 6.04	0.9859	1.02 ± 0.10	0.9874	0.17 ± 0.02	0.9989
8j	4CN-Ph	49.37 ± 4.79	0.9878	23.95 ± 2.29	0.9875	ND[h]	ND[h]	0.22 ± 0.03	0.9978
8k	5Cl–2NO_2-Ph	61.47 ± 5.93	0.9874	54.46 ± 5.59	0.9864	ND[h]	ND[h]	0.17 ± 0.06	0.9926
8l	4SO_2NH_2-Ph	42.20 ± 3.90	0.9882	27.66 ± 2.50	0.9884	3.44 ± 0.29	0.9892	0.26 ± 0.02	0.9988
8m	4COOH-Ph	55.90 ± 5.38	0.9876	37.75 ± 3.52	0.9882	5.48 ± 0.50	0.9883	0.28 ± 0.02	0.9986
AAZ[f]	–	439.17 ± 9.30	0.9990	98.28 ± 1.69	0.9992	–	–	–	–
ACR[g]	–	–	–	–	–	23.53 ± 2.72	0.9756	48.17 ± 2.34	0.9825

[a] Human carbonic anhydrase I.
[b] Human carbonic anhydrase II.
[c] α-Glycosidase.
[d] α-Amylase.
[e] Test results were expressed as means of triplicate assays ± SEM.
[f] Acetazolamide.
[g] Acarbose.
[h] Not determined.

was carried out employing the Glide application [83] [84] [85], utilizing default parameters alongside the extra precision (XP) methodology. Moreover, the efficacy of the Prime MM-GBSA [86] in predicting relative binding affinity was assessed within the framework of the VSGB energy model and the OPLS4 force field, utilizing the protein-ligand complexes derived from PDB IDs 1AZM, 3HS4, and 5NN5. Additionally, the QikProp tool and SwissADME platform [87] were harnessed to forecast the ADME characteristics of all targeted derivatives (**8a-m**) within the purview of this investigation.

2.10. Statistical study

GraphPad Prism, version 9 (GraphPad Software, La Jolla, California, USA), tailored for Macintosh systems, served as the primary analytical tool in this study. K_I values were determined using SigmaPlot, version 12 (Systat Software, San Jose, California, USA), specifically designed for Windows platforms. A comprehensive analysis was performed using the extra sum-of-squares *F* test and the Akaike Information Criterion (AIC) approach to discern the nuances in statistical measures across the datasets. Statistical significance was deemed present when the calculated *p*-value fell below the threshold of 0.05. The resulting findings were meticulously presented in a structured format denoting the mean values accompanied by their respective standard errors, encapsulated within 95 % confidence intervals.

3. Results and discussion

3.1. Chemistry

The compounds (**8a-m**) shown in Scheme 1 were prepared in six steps. Esterification step was carried out from sulfamoylbenzoicacid in ethanol with catalytic amount of sulfuric acid by refluxing for 24 h. 4-sulfonylamidebenzohydrazide was prepared with hydrazine hydrate in ethanol at 70 °C for 24 h. 4-(5-thioxo-4,5-dihydro-1,3,4-oxadiazol-2-yl) benzenesulfonamide was synthesized by reacting carbon disulfur and 4-sulfonylamide benzohydrazide in DMF in the presence of K_2CO_3. The propargylation of the compound was prepared using propargyl bromide in DMF in basic condition. The final targeted compounds (**8a-m**) were prepared by propargylated compound and arylazides in the presence of $CuSO_4$ and sodium ascorbate in DMF at 90 °C for 12 h. The structures of the targeted compounds were confirmed by the data ^{1}H NMR, ^{13}C NMR, FT-IR, and QTOF LC-MS analysis.

In the infrared spectra of compounds **8a-m**, it was possible to observe the absorptions around 3300 cm^{-1} relating to N–H. There are two peaks assigned to S═O as asymmetric and symmetric stretching which are appeared around 1300 and 1150 cm^{-1}, respectively. From the ^{1}H NMR data, the most characteristic peaks are seen as a singlet (1H) at over 8.70 ppm for the proton belongs to triazole ring, a singlet (2H) at around 7.50 ppm for NH_2, and a singlet (2H) at around 4.75 ppm for CH_2 between the triazole ring and sulfur atom. The specific carbon signal of oxadiazole ring is seen at around 165 ppm in the ^{13}C NMR spectra. All spectra and mass analyses support the structure of the synthesized compounds.

3.2. Biological evaluation

3.2.1. Inhibitory effects of the target compounds

Expanding upon the groundwork laid in our antecedent multi-target inhibition inquiries regarding both *h*CAs, α-GLY, and α-AMY [88,89], our present research endeavors encompassed a comprehensive *in vitro* examination aimed at elucidating the inhibitory efficacy of a series of novel synthesized 1,2,3-triazolylmethylthio-1,3,4-oxadiazolylbenzenesulfonamide derivatives (designated as **8a-m**) against these prominent metabolic enzymes. The evaluation protocols employed for this investigation relied upon the established spectrophotometric assays known as Verpoorte's, Tao's, and Xiao's methods, renowned for their reliability and precision in assessing *h*CAs, α-GLY, and α-AMY inhibition,

respectively. The resultant empirical observations, along with their corresponding inhibition data, have been meticulously tabulated in Table 1, furnishing a concise yet comprehensive depiction of the inhibitory potential exhibited by the investigated compounds. It is noteworthy to emphasize that acetazolamide (AAZ for *h*CAs) and acarbose (ACR for α-GLY and α-AMY), clinically employed inhibitors, were used as reference standards throughout the course of this study, facilitating comparative analysis and validation of the experimental outcomes.

Examining the inhibitory potential of the newly synthesized 1,2,3-triazolylmethylthio-1,3,4-oxadiazolylbenzenesulfonamides **8a-m** against the two disparate *h*CA isoforms in light of their structural variances unveiled intriguing findings. Concerning the cytosolic isoform *h*CA I, it was observed that sulfonamides **8a-m** exhibited potent inhibition of this isoform, with inhibition constants (K_I) ranging from 42.20 ± 3.90 nM to 217.90 ± 11.81 nM compared to the reference standard AAZ (K_I of 439.17 ± 9.30 nM). Notably, incorporating the 4-phenylsulfonamide substituent in compound **8l** manifested the most favorable inhibition constant (K_I of 42.20 ± 3.90 nM). Specifically, the compounds bearing the 4-fluorophenyl, 4-cyanophenyl, 4-carboxyphenyl, 4-chlorophenyl, 2-chlorophenyl, 5-chloro-2-nitrophenyl, 3-fluorophenyl, 4-iodoyphenyl, pentyl, 4-bromophenyl, 4-hydroxyphenyl, and phenyl, namely **8h**, **8j**, **8m**, **8f**, **8g**, **8k**, **8i**, **8d**, **8a**, **8e**, **8c**, and **8b**, respectively, displayed the low inhibitory efficacy (K_Is of 55.90 ± 5.38 nM, 56.01 ± 5.75 nM, 58.48 ± 3.39 nM, 61.47 ± 5.93 nM, 66.16 ± 6.84 nM, 69.41 ± 6.85 nM, 81.42 ± 7.37 nM, 156.60 ± 9.51 nM, 212.30 ± 13.85 nM, and 217.90 ± 11.81 nM) (Table 1).

However, it was evident that the cytosolic isoform *h*CA II was effectively suppressed by sulfonamides **8a-m**, with K_I values spanning the nanomolar range: 16.44 ± 1.53–253.70 ± 17.70 nM. Remarkably, the 4-chlorophenyl substituent of compound **8f** demonstrated superior inhibitory activity (K_I of 16.44 ± 1.53 nM) compared to the reference standard AAZ (K_I of 98.28 ± 1.69 nM). Nevertheless, the remaining derivatives, except **8b**, **8c**, and **8e**, exhibited increased inhibitory effects towards *h*CA II compared to AAZ. Additionally, compound **8b**, featuring the unsubstituted phenyl motif, displayed the lowest inhibitory activity (K_I of 253.70 ± 17.70 nM), underscoring the favorability of substituting the terminal phenyl moiety for *h*CA II inhibition. Namely, compounds **8j**, **8e**, **8l**, **8m**, **8c**, **8k**, **8i**, **8g**, and **8h** with 4-cyanophenyl, 4-bromophenyl, 4-phenylsulfonamide, 4-carboxyphenyl, 4-hydroxyphenyl, 5-chloro-2-nitrophenyl, 3-fluorophenyl, 2-chlorophenyl, and 4-fluorophenyl moieties showed the best inhibitory activities (K_Is of 23.95 ± 2.29 nM, 24.36 ± 2.10 nM, 27.66 ± 2.50 nM, 37.75 ± 3.52 nM, 42.81 ± 3.83 nM, 54.46 ± 5.59 nM, 55.11 ± 6.04 nM, 57.79 ± 4.03 nM, and 70.82 ± 4.51 nM, respectively) compared to AAZ (Table 1).

Furthermore, the findings concerning the α-GLY unveiled the capability of target sulfonamide derivatives **8a-m** to inhibit this enzyme with K_I constants in the micromolar range (0.54 ± 0.06–5.48 ± 0.50 μM) (Table 1). Compounds **8a**, **8h**, and **8g**, bearing pentyl, 4-fluorophenyl, and 2-chlorophenyl moieties, respectively, exhibited the most potent inhibitory effects (K_Is of 0.54 ± 0.06 μM, 0.61 ± 0.06 μM, and 0.98 ± 0.10 μM, respectively) compared to the reference standard ACR (K_I of 23.53 ± 2.72 μM). The introduction of the carboxy group at the 4-position of the phenyl moiety in compound **8m** resulted in the least inhibition towards α-GLY (K_I of 5.48 ± 0.50 μM). Lastly, the kinetic data presented in Table 1 divulged that the α-AMY enzyme was effectively inhibited by sulfonamides **8a-m**, with IC_{50} values in the micromolar range (0.16 ± 0.04–7.81 ± 0.51 μM). Furthermore, the results demonstrated that compound **8g**, featuring the terminal 2-chlorophenyl tail, exhibited most potent inhibition (IC_{50} of 0.16 ± 0.04 μM) to the reference standard ACR (IC_{50} of 48.17 ± 2.34 μM). Additionally, compounds **8i** and **8k**, incorporating 3-fluorophenyl and 5-chloro-2-nitrophenyl motifs, respectively, demonstrated the similar inhibitory effects (IC_{50}s of 0.17 ± 0.02 μM and 0.17 ± 0.06 μM, respectively). It is noteworthy that the bioisosteric substitution of the pentyl tail in sulfonamide **8a** and a phenyl motif in **8b** resulted in a slight decrease in inhibition towards the α-AMY; IC_{50}s of 7.81 ± 0.51 μM and 1.15 ± 0.16 μM, respectively.

Table 2
The radical scavenging activity of novel 1,2,3-triazolylmethylthio-1,3,4-oxadiazolylbenzenesulfonamides (**8a-m**) and standard antioxidants BHT and trolox.

Compound ID	DPPH· Scavenging[a] [20 μg/ml]	$ABTS^{+}$· Scavenging[a] [20 μg/ml]
8a	5.47 ± 2.80	37.13 ± 3.47
8b	ND[d]	28.31 ± 2.53
8c	26.67 ± 3.21	30.88 ± 3.31
8d	ND[d]	24.27 ± 2.98
8e	7.22 ± 1.43	21.69 ± 2.13
8f	ND[d]	24.27 ± 1.76
8g	ND[d]	36.03 ± 3.28
8h	2.81 ± 1.04	28.68 ± 2.89
8i	ND[d]	32.72 ± 2.06
8j	2.96 ± 0.79	29.04 ± 1.16
8k	ND[d]	34.56 ± 2.76
8l	ND[d]	ND[d]
8m	ND[d]	ND[d]
BHT[b]	45.37 ± 4.43	39.34 ± 2.39[e]
TRX[c]	44.76 ± 3.65	55.15 ± 5.85[d]

[a] Test results were expressed as means of triplicate assays ± SEM.
[b] Butylated hydroxytoluene.
[c] Trolox.
[d] Not determined.
[e] At a concentration of 2 μg/ml.

3.2.2. *DPPH· and $ABTS^{+}$· radical scavenging activity of the target compounds*

Given the centrality of oxidative stress in the pathogenesis of generally metabolic diseases, a rigorous investigation was undertaken to scrutinize the antioxidant potential of the newly devised and synthesized 1,2,3-triazolylmethylthio-1,3,4-oxadiazolylbenzenesulfonamide derivatives (**8a-m**). The primary focus of the inquiry was to assess their efficacy in scavenging DPPH· and $ABTS^{+}$· radicals, which represent the benchmark techniques for evaluating antioxidant capacity. To ensure comprehensive evaluation, these derivatives (**8a-m**) were tested alongside butylated hydroxytoluene (BHT) and trolox (TRX), a water-soluble analogue of vitamin E widely recognized as a standard positive control for antioxidants. The results, elucidated in Table 2, provided crucial insights.

As anticipated, the scavenging efficacy of the novel compounds exhibited a discernible dependence on their constituent functional moieties. Notably, compounds **8b**, **8d**, **8f-g**, **8i**, and **8k-m** (for DPPH·) and **8l-m** (for $ABTS^{+}$·) were determined not to demonstrate radical removal capability (IC_{50} > 160 μM, data not presented), while the antioxidative potential of the remaining sulfonamides exhibited variability with the presence of various electron-withdrawing and/or -donating functional groups in their structures. Overall, the majority of compounds (except for **8l** and **8m**) under examination exhibited potent $ABTS^{+}$· scavenging activity with IC_{50} values ranging from 21.69 ± 2.13 to 37.13 ± 3.47 μM compared to standard positive controls, BHT and Trolox. Noteworthy among these findings is the superior performance of compounds **8a** (5.47 ± 2.80 μM), **8c** (26.67 ± 3.21 μM), **8e** (7.22 ± 1.43 μM), **8h** (2.81 ± 1.04 μM), and **8j** (2.96 ± 0.79 μM) with pentyl, 4-hydroxyphenyl, 4-bromophenyl, 4-fluorophenyl, and 4-cyanophenyl moieties, which outperformed even the BHT and Trolox (IC_{50}s of 45.37 ± 4.43 μM and 44.76 ± 3.65 μM, respectively) against DPPH·.

3.3. *In silico study*

3.3.1. *Molecular docking study*

A comprehensive molecular docking analysis was conducted to provide *in silico* insights into the measured *in vitro* inhibition study of *h*CA II and α-GLY, juxtaposed with *h*CA I, in accordance with our strategic design approach. The docking experiments were meticulously executed employing the X-ray crystallographic structures for both *h*CA I,

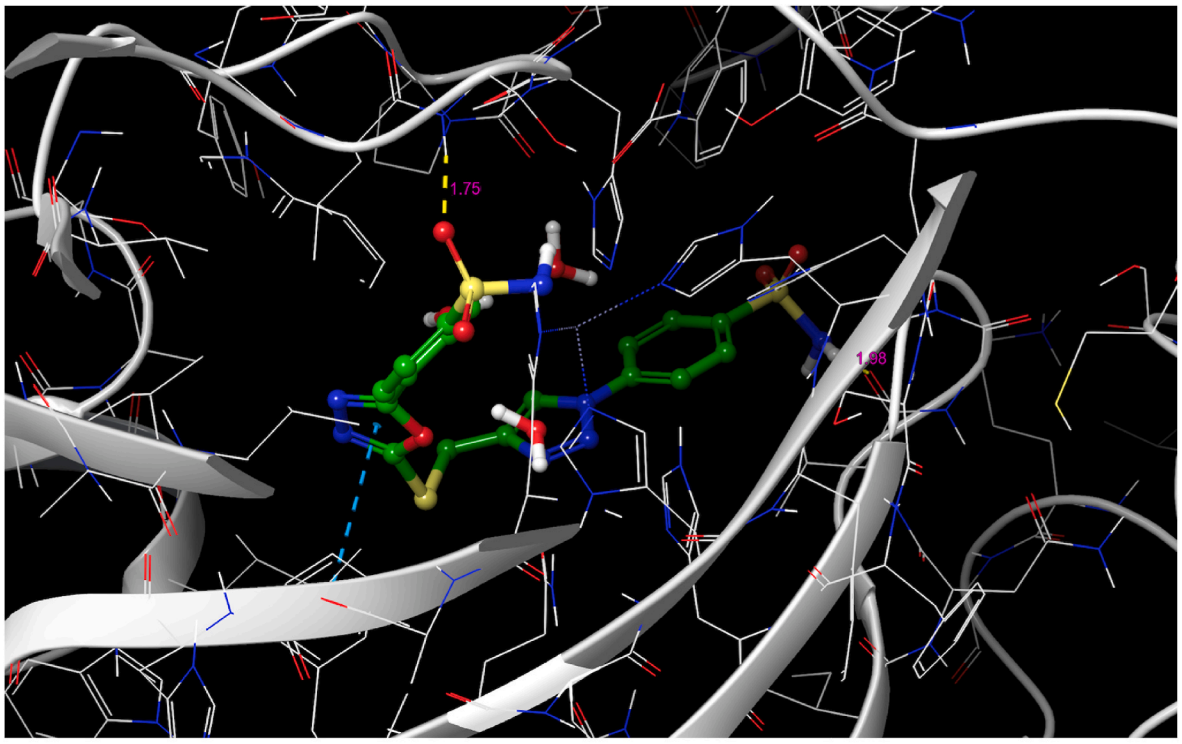

A

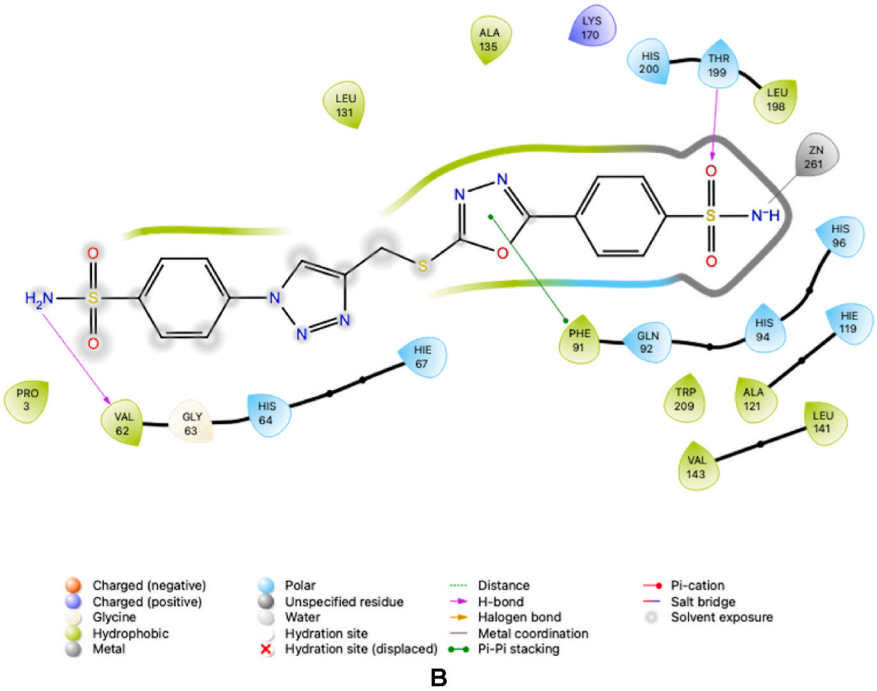

B

Fig. 3. Illustrates the molecular docking procedure performed on the *h*CA I isoform (PDB ID 1AZM) with 4-[4-({[5-(4-sulfamoylphenyl)-1,3,4-oxadiazol-2-yl]thio}methyl)-1*H*-1,2,3-triazol-1-yl]benzenesulfonamide (**8l**), resulting in the 3D docking pose of compound **8l** within the binding pocket of 1AZM, as depicted in panel A. Subsequently, a 2D interaction diagram (shown in panel B) was generated to elucidate the specific interactions between 1AZM and compound **8l**. The 3D diagram highlights hydrogen bonds and pi-pi stacking interactions, represented by yellow and blue dashed lines, respectively, focusing on the interacting amino acids to ensure clarity.

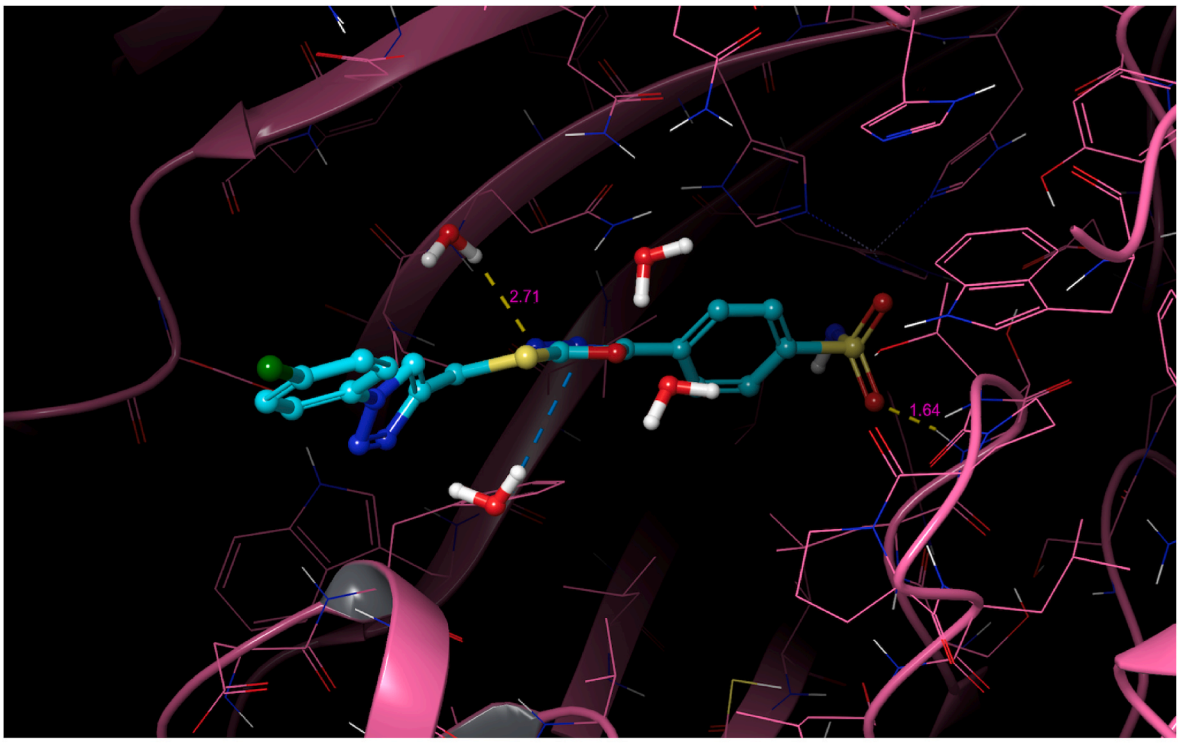

A

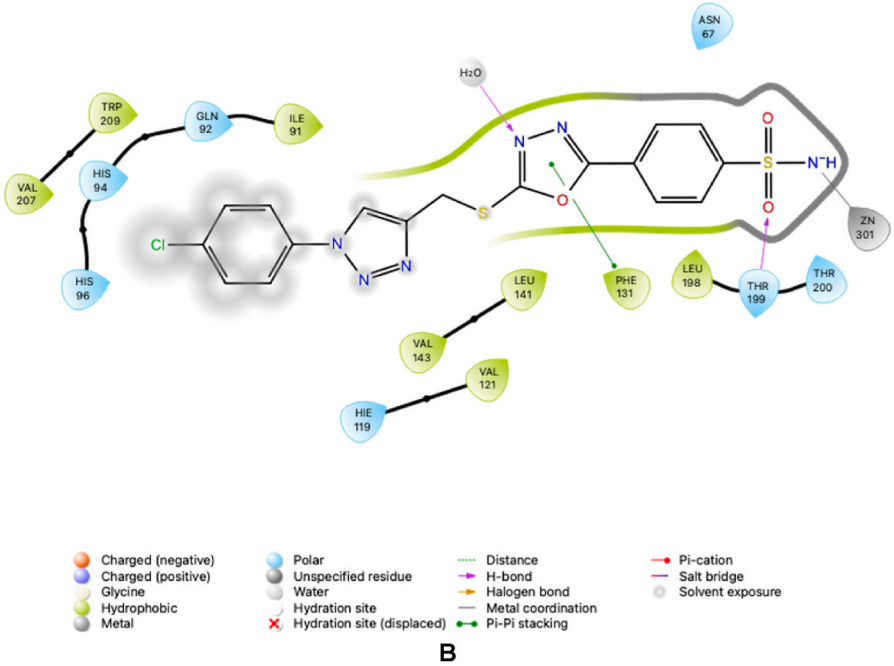

B

Fig. 4. Illustrates the molecular docking procedure performed on the *h*CA II isoform (PDB ID 3HS4) with 4-[5-({[1-(4-chlorophenyl)-1*H*-1,2,3-triazol-4-yl]methyl} thio)-1,3,4-oxadiazol-2-yl]benzenesulfonamid (**8f**), resulting in the 3D docking pose of compound **8f** within the binding pocket of 3HS4, as depicted in panel A. Subsequently, a 2D interaction diagram (shown in panel B) was generated to elucidate the specific interactions between 3HS4 and compound **8f**. The 3D diagram highlights hydrogen bonds and pi-pi stacking interactions, represented by yellow and blue dashed lines, respectively, focusing on the interacting amino acids to ensure clarity.

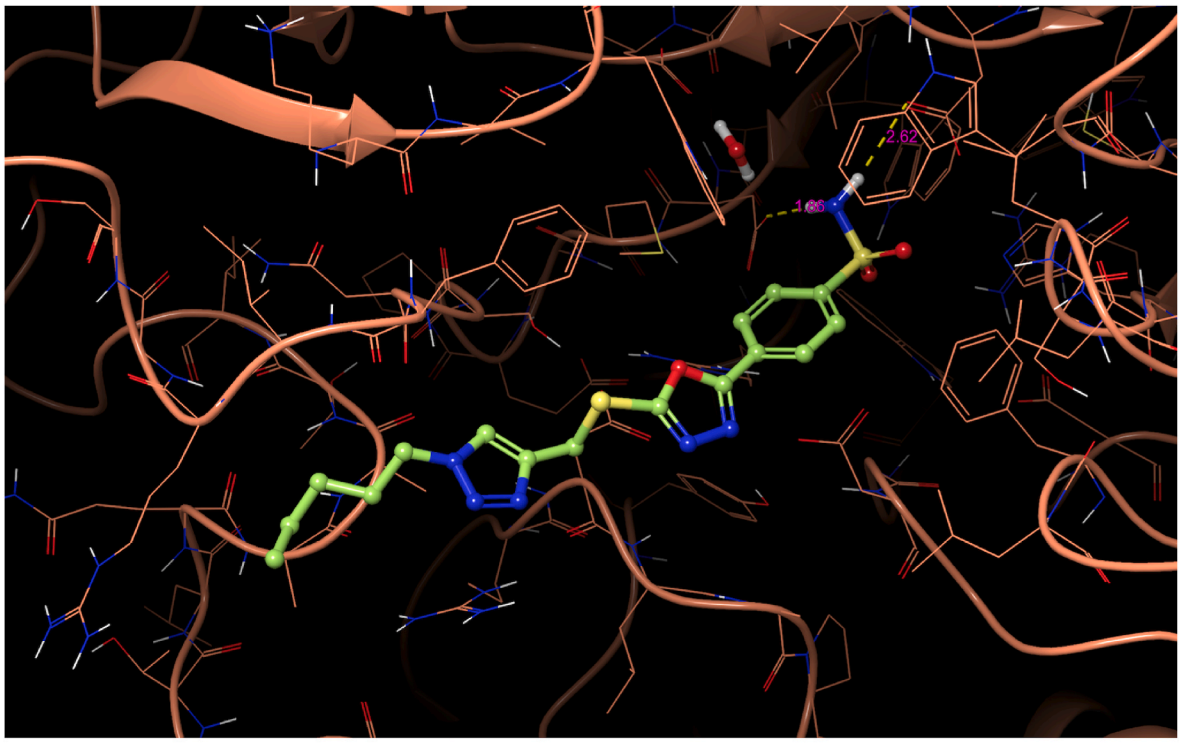

A

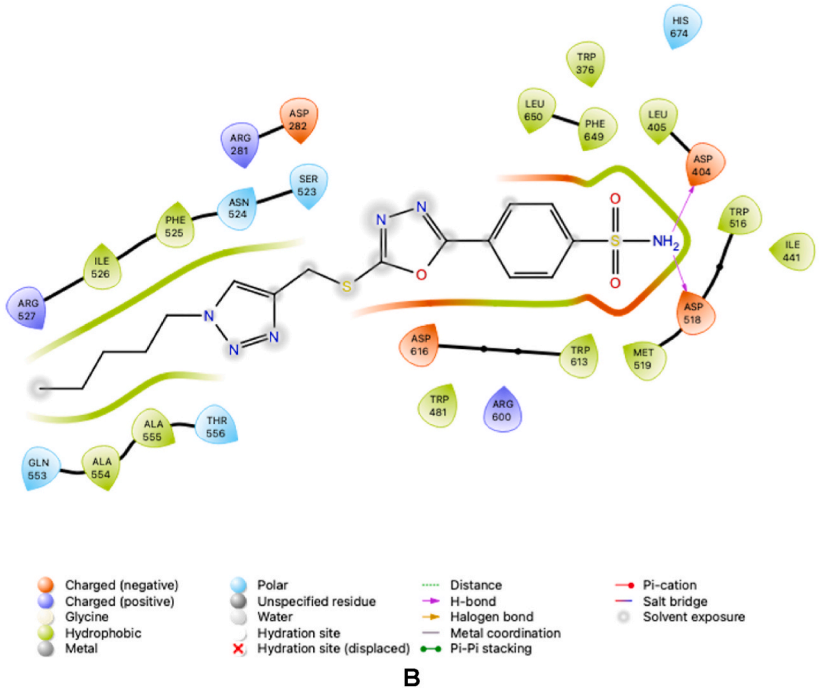

B

Fig. 5. Illustrates the molecular docking procedure performed on the α-GLY isoform (PDB ID 5NN8) with 4-[5-{[(1-pentyl-1*H*-1,2,3-triazol-4-yl)methyl]thio}-1,3,4-oxadiazol-2-yl]benzenesulfonamide (**8a**), resulting in the 3D docking pose of compound **8a** within the binding pocket of 5NN8, as depicted in panel A. Subsequently, a 2D interaction diagram (shown in panel B) was generated to elucidate the specific interactions between 5NN8 and compound **8a**. The 3D diagram highlights hydrogen bonds, represented by yellow dashed lines, focusing on the interacting amino acids to ensure clarity.

*h*CA II, and α-GLY, as cataloged by their respective Protein Data Bank (PDB) IDs: 1AZM, 3HS4, and 5NN8, respectively. To validate the robustness of the docking protocol, pose-retrieval experiments were conducted using the co-crystal ligands AAZ (for *h*CAs) and ACR (for α-GLY) against their corresponding X-ray coordinates. This procedure verified the fidelity and accuracy of the docking setup intended for pose prediction. Notably, all pose retrieval experiments yielded root-mean-square deviation (RMSD) values of less than 1.5 Å, indicative of the high precision and reliability of the docking methodology employed in our study. Upon elucidating the docking poses of the novel 1,2,3-

triazolylmethylthio-1,3,4-oxadiazolylbenzenesulfonamides (**8a-m**), it becomes apparent that the most potent competitive compounds (**8l** for *h*CA I, **8f** for *h*CA II, and **8a** for α-GLY) engender comparable interactions within the binding sites of *h*CAs and α-GLY, as illustrated in Figs. 3–5.

Notably, these sulfonamides are positioned in close proximity to the Zn^{2+} ion, suggesting favorable coordination with the *h*CAs. Moreover, the benzenesulfonamide groups of compounds **8l** (distance of 1.75 Å) and **8f** (distance of 1.64 Å) form hydrogen-bonding interactions with Thr199, indicating robust *in silico* binding of the sulfonamide head groups. Furthermore, the amino moiety of the other sulfonamide group exhibits hydrogen-bonding interaction with the side chain of Val62 in *h*CA I (distance of 1.98 Å), further augmenting the stability of the binding configuration. Concurrently, the oxadiazole rings of compounds **8l** and **8f** make pi-pi stacking with residues Phe91 and Phe131, respectively, thus primarily fostering favorable hydrophobic contacts, as depicted in Figs. 3 and 4. The proposed binding orientations of compound **8a** exhibit a congruent interaction profile within the binding site of α-GLY and display hydrogen-bonding interactions with Asp404 and Asp518 (distances of 2.62 and 1.86 Å, respectively), as depicted in Fig. 5. Herein, it is noteworthy that the elongation of the linker can precipitate other effects, such as enthalpy-entropy compensation, wherein favorable interactions counterbalance the unfavorable internal entropy. This phenomenon can elucidate the higher inhibition effect of 8a relative to other compounds in this series. Theoretically, the introduction of more flexible congeners has the potential to augment the internal entropy of the derivatives, albeit this augmentation may exert a negative influence on their binding affinity towards α-GLY.

3.3.2. *Physicochemical properties and ADME prediction*

Determining *in silico* the physicochemical and pharmacokinetic attributes of targeted compounds is a pivotal endeavor in novel drug development. Thus, to assess the drug-likeness of the novel synthesized 1,2,3-triazolylmethylthio-1,3,4-oxadiazolylbenzenesulfonamide derivatives (**8a-m**), *in silico* physiochemical properties and ADME (Absorption, Distribution, Metabolism, and Excretion) predictions were conducted for all compounds employing the QikProp tool [90] and SwissADME platform [91] with outcomes delineated in Tables S1–S4 and Fig. S1. Complying with the parameters of Lipinski's Rule of Five [92] and Jorgensen's Rule of Three [93], a cardinal framework for gauging drug-likeness and the likelihood of favorable oral absorption, the analysis of active compounds (Table S1) revealed some have only a solitary violation, a permissible deviation, indicative of their potential to exhibit drug-like characteristics and feasibly manifest oral bioactivity. Concurrent with Lipinski's and Jorgensen's guidelines, the assessment of ADME parameters for these compounds was executed, with findings detailed in Tables S2–S4. Consequently, the ensemble of active compounds demonstrated commendable *in silico* physicochemical attributes and ADME projections, suggesting their promising candidacy as orally active lead molecules.

4. Conclusions

Within the scope of this investigation, we have unveiled a novel series of 1,2,3-triazolylmethylthio-1,3,4-oxadiazolylbenzenesulfonamide derivatives (**8a-m**), meticulously crafted through design and synthesis and subjected to thorough biological assessment. These compounds were evaluated for their inhibitory potential against *h*CA I, *h*CA II, α-GLY, and α-AMY, pivotal enzymes implicated in metabolic disorders. Our findings illuminate a spectrum of inhibitory effects across the synthesized compounds, particularly noteworthy in their impact on *h*CA I/II, α-GLY, and α-AMY. Remarkably, all synthesized sulfonamides exhibited notable inhibition of *h*CA I, with K_I ranging from 42.20 ± 3.90 nM to 217.90 ± 11.81 nM, showcasing superior potency compared to the reference standard AAZ (K_I of 439.17 ± 9.30 nM). Evaluation against *h*CA II revealed potent inhibition by most derivatives, with K_I constants spanning the nanomolar range (16.44 ± 1.53 nM-70.82 ± 4.51 nM). However, specific compounds (**8a-b** and **8d**) demonstrated reduced inhibitory potency relative to the reference drug AAZ. Notably, compounds **8c** and **8e** exhibited significant selectivity towards *h*CA II, underscoring the potential for isoform-specific targeting. Furthermore, our investigations revealed potent inhibition against α-GLY and α-AMY, pivotal in diabetes mellitus pathology. The synthesized compounds exhibited impressive inhibition profiles against α-GLY (K_Is of 0.54 ± 0.06 μM to 5.48 ± 0.50 μM) and α-AMY (IC_{50}s of 0.16 ± 0.04 μM to 7.81 ± 0.51 μM), surpassing the efficacy of the reference standard ACR. Additionally, the compounds were evaluated for their antioxidant activity through DPPH· and $ABTS^{+}$· radical scavenging assays. Molecular docking studies provided further insights into the inhibitory mechanisms, elucidating the interactions within the active sites of *h*CA I/II, α-GLY, and α-AMY. In summary, our study underscores the potential of the synthesized sulfonamide derivatives as potent multi-target inhibitors against key enzymes implicated in metabolic diseases, offering valuable prospects for therapeutic intervention and warranting further exploration in drug development endeavors.

Data availability

Data is provided within the manuscript or supplementary information files.

CRediT authorship contribution statement

Özcan Güleç: Validation, Investigation, Formal analysis. **Cüneyt Türkeş:** Writing – original draft, Validation, Methodology, Investigation, Formal analysis, Conceptualization. **Mustafa Arslan:** Writing – original draft, Validation, Methodology, Investigation, Formal analysis, Conceptualization. **Mesut Işık:** Validation, Investigation, Formal analysis. **Yeliz Demir:** Validation, Investigation, Formal analysis. **Hatice Esra Duran:** Validation, Investigation, Formal analysis. **Muhammet Fırat:** Formal analysis. **Ömer İrfan Küfrevioğlu:** Methodology, Conceptualization. **Şükrü Beydemir:** Methodology, Funding acquisition, Conceptualization.

Declaration of competing interest

The authors declare no conflict of interest.

Acknowledgement

Author Özcan Güleç is a 100/2000 The Council of Higher Education (CoHE) Ph.D. Scholar in the Organic Smart and Innovative Materials Subsection. This work was supported by the Research Fund of Anadolu University, Turkey (grant number 2102S003).

Appendix A. Supplementary data

Supplementary data to this article can be found online at https://doi.org/10.1016/j.abb.2024.110099.

References

[1] A. Talevi, C. L Bellera, M. Di Ianni, M. Gantner, L. E Bruno-Blanch, E. A Castro, CNS drug development-lost in translation? Mini-Rev. Med. Chem. 12 (10) (2012) 959–970, https://doi.org/10.2174/138955712802762356.
[2] H. Zheng, M. Fridkin, M. Youdim, From single target to multitarget/network therapeutics in Alzheimer's therapy, Pharmaceuticals 7 (2) (2014) 113–135, https://doi.org/10.3390/ph7020113.
[3] A. Sadri, Is target-based drug discovery efficient? Discovery and "off-target" mechanisms of all drugs, J. Med. Chem. 66 (18) (2023) 12651–12677, https://doi.org/10.1021/acs.jmedchem.2c01737.
[4] S.J. Virolainen, A. VonHandorf, K.C.M.F. Viel, M.T. Weirauch, L.C. Kottyan, Gene–environment interactions and their impact on human health, Gene Immun. 24 (1) (2023) 1–11, https://doi.org/10.1038/s41435-022-00192-6.

[5] A. Artasensi, A. Pedretti, G. Vistoli, L. Fumagalli, Type 2 diabetes mellitus: a review of multi-target drugs, Molecules 25 (8) (2020) 1987, https://doi.org/10.3390/molecules25081987.

[6] A. Bonardi, A. Nocentini, S. Bua, J. Combs, C. Lomelino, J. Andring, L. Lucarini, S. Sgambellone, E. Masini, R. McKenna, P. Gratteri, C.T. Supuran, Sulfonamide inhibitors of human carbonic anhydrases designed through a three-tails approach: improving ligand/isoform matching and selectivity of action, J. Med. Chem. 63 (13) (2020) 7422–7444, https://doi.org/10.1021/acs.jmedchem.0c00733.

[7] H. Xiang, Y. Shao, N. Gao, X. Lu, W. Chu, N. An, C. Tan, X. Zheng, Y. Gao, The influence of bromide on the degradation of sulfonamides in UV/free chlorine treatment: degradation mechanism, DBPs formation and toxicity assessment, Chem. Eng. J. (Lausanne) 362 (2019) 692–701, https://doi.org/10.1016/j.cej.2019.01.079.

[8] L.H. Mitchell, P.A. Boriack-Sjodin, S. Smith, M. Thomenius, N. Rioux, M. Munchhof, J.E. Mills, C. Klaus, J. Totman, T.V. Riera, A. Raimondi, S.L. Jacques, K. West, M. Foley, N.J. Waters, K.W. Kuntz, T.J. Wigle, M.P. Scott, R.A. Copeland, J.J. Smith, R. Chesworth, Novel oxindole sulfonamides and sulfamides: EPZ031686, the first orally bioavailable small molecule SMYD3 inhibitor, ACS Med. Chem. Lett. 7 (2) (2016) 134–138, https://doi.org/10.1021/acsmedchemlett.5b00272.

[9] A.K. Pandey, A. Kumar, S.K. Srivastava, Blue light-induced coupling of N-hydroxy sulfonamides: an efficient and green approach to symmetrical thiosulfonates, Russ. J. Org. Chem. 58 (6) (2022) 844–849, https://doi.org/10.1134/S1070428022060136.

[10] D.S. Daniels, A.S. Jones, A.L. Thompson, R.S. Paton, E.A. Anderson, Ligand bite angle-dependent palladium-catalyzed cyclization of propargylic carbonates to 2-alkynyl azacycles or cyclic dienamides, Angew. Chem. 126 (7) (2014) 1946–1951, https://doi.org/10.1002/ange.201309162.

[11] H. Azevedo-Barbosa, D.F. Dias, L.L. Franco, J.A. Hawkes, D.T. Carvalho, From antibacterial to antitumour agents: a brief review on the chemical and medicinal aspects of sulfonamides, Mini-Rev. Med. Chem. 20 (19) (2020) 2052–2066, https://doi.org/10.2174/1389557520666200905125738.

[12] A.-M. Alaa, A. Angeli, A.S. El-Azab, M.E. Hammouda, M.A. El-Sherbeny, C. T. Supuran, Synthesis and anti-inflammatory activity of sulfonamides and carboxylates incorporating trimellitimides: dual cyclooxygenase/carbonic anhydrase inhibitory actions, Bioorg. Chem. 84 (2019) 260–268, https://doi.org/10.1016/j.bioorg.2018.11.033.

[13] M.Y. Moskalik, Sulfonamides with heterocyclic periphery as antiviral agents, Molecules 28 (1) (2022) 51, https://doi.org/10.3390/molecules28010051.

[14] M.S. Ayoup, N. Khaled, H. Abdel-Hamid, D.A. Ghareeb, S.A. Nasr, A. Omer, A. Sonousi, A.E. Kassab, A.S. Eltaweil, Novel sulfonamide derivatives as multitarget antidiabetic agents: design, synthesis, and biological evaluation, RSC Adv. 14 (11) (2024) 7664–7675, https://doi.org/10.1039/D4RA01060D.

[15] C.T. Supuran, How many carbonic anhydrase inhibition mechanisms exist? J. Enzym. Inhib. Med. Chem. 31 (3) (2016) 345–360, https://doi.org/10.3109/14756366.2015.1122001.

[16] G. Verma, M.F. Khan, W. Akhtar, M.M. Alam, M. Akhter, M. Shaquiquzzaman, A review exploring therapeutic worth of 1, 3, 4-oxadiazole tailored compounds, Mini-Rev. Med. Chem. 19 (6) (2019) 477–509, https://doi.org/10.2174/1389557518666181015152433.

[17] S.S. Tawfik, A.A. Farahat, M. A-A El-Sayed, A.S. Tantawy, O. Bagato, M.A. Ali, Synthesis and anti-influenza activity of novel thiadiazole, oxadiazole and triazole based scaffolds, Lett. Drug Des. Discovery 15 (4) (2018) 363–374, https://doi.org/10.2174/1570180814666170512122832.

[18] M.M. Alam, A.S. Almalki, T. Neamatallah, N.M. Ali, A.M. Malebari, S. Nazreen, Synthesis of new 1, 3, 4-oxadiazole-incorporated 1, 2, 3-triazole moieties as potential anticancer agents targeting thymidylate synthase and their docking studies, Pharmaceuticals 13 (11) (2020) 390, https://doi.org/10.3390/ph13110390.

[19] T. Glomb, P. Świątek, Antimicrobial activity of 1, 3, 4-oxadiazole derivatives, Int. J. Mol. Sci. 22 (13) (2021) 6979, https://doi.org/10.3390/ijms22136979.

[20] B. Zhang, Comprehensive review on the anti-bacterial activity of 1, 2, 3-triazole hybrids, Eur. J. Med. Chem. 168 (2019) 357–372, https://doi.org/10.1016/j.ejmech.2019.02.055.

[21] M.Y. Wani, A. Ahmad, R.A. Shiekh, K.J. Al-Ghamdi, A.J. Sobral, Imidazole clubbed 1, 3, 4-oxadiazole derivatives as potential antifungal agents, Bioorg. Med. Chem. 23 (15) (2015) 4172–4180, https://doi.org/10.1016/j.bmc.2015.06.053.

[22] N.G. Aher, V.S. Pore, N.N. Mishra, A. Kumar, P.K. Shukla, A. Sharma, M.K. Bhat, Synthesis and antifungal activity of 1, 2, 3-triazole containing fluconazole analogues, Bioorg. Med. Chem. Lett 19 (3) (2009) 759–763, https://doi.org/10.1016/j.bmcl.2008.12.026.

[23] H.S. Abd-Ellah, M. Abdel-Aziz, M.E. Shoman, E.A. Beshr, T.S. Kaoud, A.-S. F. Ahmed, Novel 1, 3, 4-oxadiazole/oxime hybrids: synthesis, docking studies and investigation of anti-inflammatory, ulcerogenic liability and analgesic activities, Bioorg. Chem. 69 (2016) 48–63, https://doi.org/10.1016/j.bioorg.2016.09.005.

[24] K.K. Angajala, S. Vianala, R. Macha, M. Raghavender, M.K. Thupurani, P.J. Pathi, Synthesis, anti-inflammatory, bactericidal activities and docking studies of novel 1,2,3-triazoles derived from ibuprofen using click chemistry, SpringerPlus 5 (1) (2016) 423, https://doi.org/10.1186/s40064-016-2052-5.

[25] M.M. Hamoud, N.A. Osman, S. Rezq, H.A. Abd El-wahab, A.E. Hassan, H.A. Abdel-Fattah, D.G. Romero, A.M. Ghanim, Design and synthesis of novel 1, 3, 4-oxadiazole and 1, 2, 4-triazole derivatives as cyclooxygenase-2 inhibitors with anti-inflammatory and antioxidant activity in LPS-stimulated RAW264. 7 macrophages, Bioorg. Chem. 124 (2022) 105808, https://doi.org/10.1016/j.bioorg.2022.105808.

[26] M.M. Alam, 1, 2, 3-Triazole hybrids as anticancer agents: a review, Arch. Pharm. (Weinheim, Ger.) 355 (1) (2022) 2100158.

[27] F. Peng, T. Liu, Q. Wang, F. Liu, X. Cao, J. Yang, L. Liu, C. Xie, W. Xue, Antibacterial and antiviral activities of 1,3,4-oxadiazole thioether 4H-Chromen-4-one derivatives, J. Agric. Food Chem. 69 (37) (2021) 11085–11094, https://doi.org/10.1021/acs.jafc.1c03755.

[28] L.S. Feng, M.J. Zheng, F. Zhao, D. Liu, 1, 2, 3-Triazole hybrids with anti-HIV-1 activity, Arch. Pharm. (Weinheim, Ger.) 354 (1) (2021) 2000163, https://doi.org/10.1002/ardp.202000163.

[29] P. Rayam, N. Polkam, B. Kummari, V. Banothu, D. Gandamalla, N.R. Yellu, J. S. Anireddy, Synthesis and biological evaluation of new ibuprofen-1, 3, 4-oxadiazole-1, 2, 3-triazole hybrids, J. Heterocycl. Chem. 56 (1) (2019) 296–305, https://doi.org/10.1002/jhet.3409.

[30] M.A. Mahmoud, A.F. Mohammed, O.I. Salem, H.A. Gomaa, B.G. Youssif, New 1, 3, 4-oxadiazoles linked with the 1, 2, 3-triazole moiety as antiproliferative agents targeting the EGFR tyrosine kinase, Arch. Pharm. (Weinheim, Ger.) 355 (6) (2022) 2200009, https://doi.org/10.1002/ardp.202200009.

[31] F.-F. Yang, J.-Z. Zhou, X.-L. Xu, T. Hu, J.-Q. Liu, Y.-X. Wu, B. Wei, L.-Y. Ma, Discovery of 1, 3, 4-oxadiazole derivatives containing a bisamide moiety as a novel class of potential cardioprotective agents, Eur. J. Med. Chem. 239 (2022) 114526, https://doi.org/10.1016/j.ejmech.2022.114526.

[32] S. Wang, H. Liu, X. Wang, K. Lei, G. Li, J. Li, R. Liu, Z. Quan, Synthesis of 1, 3, 4-oxadiazole derivatives with anticonvulsant activity and their binding to the GABAA receptor, Eur. J. Med. Chem. 206 (2020) 112672, https://doi.org/10.1016/j.ejmech.2020.112672.

[33] S.V. Akolkar, A.A. Nagargoje, M.H. Shaikh, M.Z. Warshagha, J.N. Sangshetti, M. G. Damale, B.B. Shingate, New N-phenylacetamide-linked 1, 2, 3-triazole-tethered coumarin conjugates: synthesis, bioevaluation, and molecular docking study, Arch. Pharm. (Weinheim, Ger.) 353 (11) (2020) 2000164, https://doi.org/10.1002/ardp.202000164.

[34] C.S. De Oliveira, B.F. Lira, J.M. Barbosa-Filho, J.G.F. Lorenzo, P.F. de Athayde-Filho, Synthetic approaches and pharmacological activity of 1, 3, 4-oxadiazoles: a review of the literature from 2000–2012, Molecules 17 (9) (2012) 10192–10231, https://doi.org/10.3390/molecules170910192.

[35] M.A. Abdelgawad, S.N.A. Bukhari, A. Musa, M. Elmowafy, A.A. Nayl, A.H. El-Ghorab, M.S. Abdel-Bakky, H.A. Omar, N.H. Alotaibi, H.M. Hassan, Phthalazone tethered 1, 2, 3-triazole conjugates: in silico molecular docking studies, synthesis, in vitro antiproliferative, and kinase inhibitory activities, Bioorg. Chem. 133 (2023) 106404, https://doi.org/10.1016/j.bioorg.2023.106404.

[36] V. Sharma, R. Kumar, A. Angeli, C.T. Supuran, P.K. Sharma, Tail approach synthesis of novel benzenesulfonamides incorporating 1, 3, 4-oxadiazole hybrids as potent inhibitor of carbonic anhydrase I, II, IX, and XII isoenzymes, Eur. J. Med. Chem. 193 (2020) 112219, https://doi.org/10.1016/j.ejmech.2020.112219.

[37] R.S. Gani, A.K. Kudva, K. Timanagouda, S.B.H. Mujawar, S.D. Joshi, S.V. Raghu, Synthesis of novel 5-(2, 5-bis (2, 2, 2-trifluoroethoxy) phenyl)-1, 3, 4-oxadiazole-2-thiol derivatives as potential glucosidase inhibitors, Bioorg. Chem. 114 (2021) 105046, https://doi.org/10.1016/j.bioorg.2021.105046.

[38] S.K. Avula, A. Khan, N.U. Rehman, M.U. Anwar, Z. Al-Abri, A. Wadood, M. Riaz, R. Csuk, A. Al-Harrasi, Synthesis of 1H-1, 2, 3-triazole derivatives as new α-glucosidase inhibitors and their molecular docking studies, Bioorg. Chem. 81 (2018) 98–106, https://doi.org/10.1016/j.bioorg.2018.08.008.

[39] S.S. Hamdani, B.A. Khan, M.N. Ahmed, S. Hameed, K. Akhter, K. Ayub, T. Mahmood, Synthesis, crystal structures, computational studies and α-amylase inhibition of three novel 1, 3, 4-oxadiazole derivatives, J. Mol. Struct. 1200 (2020) 127085, https://doi.org/10.1016/j.molstruc.2019.127085.

[40] E.O. Yeye, K.M. Khan, S. Chigurupati, A. Wadood, A.U. Rehman, S. Perveen, M. K. Maharajan, S. Shamim, S. Hameed, S.A. Aboaba, Syntheses, in vitro α-amylase and α-glucosidase dual inhibitory activities of 4-amino-1, 2, 4-triazole derivatives their molecular docking and kinetic studies, Bioorg. Med. Chem. 28 (11) (2020) 115467, https://doi.org/10.1016/j.bmc.2020.115467.

[41] E. Güzel, Ü.M. Koçyiğit, P. Taslimi, İ. Gülçin, S. Erkan, M. Nebioğlu, B.S. Arslan, İ. Şişman, Phthalocyanine complexes with (4-isopropylbenzyl) oxy substituents: preparation and evaluation of anti-carbonic anhydrase, anticholinesterase enzymes and molecular docking studies, J. Biomol. Struct. Dyn. 40 (2) (2022) 733–741, https://doi.org/10.1080/07391102.2020.1818623.

[42] M. Şentürk, İ. Gülçin, A. Daştan, Ö.İ. Küfrevioğlu, C.T. Supuran, Carbonic anhydrase inhibitors. Inhibition of human erythrocyte isozymes I and II with a series of antioxidant phenols, Bioorg. Med. Chem. 17 (8) (2009) 3207–3211, https://doi.org/10.1016/j.bmc.2009.01.067.

[43] F. Topal, I. Gulcin, A. Dastan, M. Guney, Novel eugenol derivatives: potent acetylcholinesterase and carbonic anhydrase inhibitors, Int. J. Biol. Macromol. 94 (2017) 845–851, https://doi.org/10.1016/j.ijbiomac.2016.10.096.

[44] A.G. Uslu, T.G. Maz, A. Nocentini, E. Banoglu, C.T. Supuran, B. Çalışkan, Benzimidazole derivatives as potent and isoform selective tumor-associated carbonic anhydrase IX/XII inhibitors, Bioorg. Chem. 95 (2020) 103544, https://doi.org/10.1016/j.bioorg.2019.103544.

[45] E. Dilek, S. Caglar, N. Dogancay, B. Caglar, O. Sahin, A. Tabak, Synthesis, crystal structure, spectroscopy, thermal properties and carbonic anhydrase activities of new metal (II) complexes with mefenamic acid and picoline derivatives, J. Coord. Chem. 70 (16) (2017) 2833–2852, https://doi.org/10.1080/00958972.2017.1366996.

[46] Z. Alım, N. Kılınç, M.M. İşgör, B. Şengül, Ş. Beydemir, Some anti-inflammatory agents inhibit esterase activities of human carbonic anhydrase isoforms I and II: an in vitro study, Chem. Biol. Drug Des. 86 (4) (2015) 857–863, https://doi.org/10.1111/cbdd.12561.

[47] Z. Alim, 1H-indazole molecules reduced the activity of human erythrocytes carbonic anhydrase I and II isoenzymes, J. Biochem. Mol. Toxicol. 32 (9) (2018) e22194, https://doi.org/10.1002/jbt.22194.
[48] İ. Gulçin, P. Taslimi, Sulfonamide inhibitors: a patent review 2013-present, Expert Opin. Ther. Pat. 28 (7) (2018) 541–549, https://doi.org/10.1080/13543776.2018.1487400.
[49] J.E. Combs, J.T. Andring, R. McKenna, Neutron crystallographic studies of carbonic anhydrase, Methods Enzymol. (2020) 281–309. Elsevier.
[50] S. Bayindir, C. Caglayan, M. Karaman, İ. Gülcin, The green synthesis and molecular docking of novel N-substituted rhodanines as effective inhibitors for carbonic anhydrase and acetylcholinesterase enzymes, Bioorg. Chem. 90 (2019) 103096, https://doi.org/10.1016/j.bioorg.2019.103096.
[51] C.T. Supuran, A simple yet multifaceted 90 years old, evergreen enzyme: carbonic anhydrase, its inhibition and activation, Bioorg. Med. Chem. Lett (2023) 129411, https://doi.org/10.1016/j.bmcl.2023.129411.
[52] P. Taslimi, K. Turhan, F. Türkan, H.S. Karaman, Z. Turgut, I. Gulcin, Cholinesterases, α-glycosidase, and carbonic anhydrase inhibition properties of 1H-pyrazolo [1, 2-b] phthalazine-5, 10-dione derivatives: synthetic analogues for the treatment of Alzheimer's disease and diabetes mellitus, Bioorg. Chem. 97 (2020) 103647, https://doi.org/10.1016/j.bioorg.2020.103647.
[53] S. Akocak, N. Lolak, S. Bua, I. Turel, C.T. Supuran, Synthesis and biological evaluation of novel N, N′-diaryl cyanoguanidines acting as potent and selective carbonic anhydrase II inhibitors, Bioorg. Chem. 77 (2018) 245–251, https://doi.org/10.1016/j.bioorg.2018.01.022.
[54] N. Lolak, S. Akocak, S. Bua, M. Koca, C.T. Supuran, Design and synthesis of novel 1, 3-diaryltriazene-substituted sulfonamides as potent and selective carbonic anhydrase II inhibitors, Bioorg. Chem. 77 (2018) 542–547, https://doi.org/10.1016/j.bioorg.2018.02.015.
[55] A. Nocentini, A. Angeli, F. Carta, J.-Y. Winum, R. Zalubovskis, S. Carradori, C. Capasso, W.A. Donald, C.T. Supuran, Reconsidering anion inhibitors in the general context of drug design studies of modulators of activity of the classical enzyme carbonic anhydrase, J. Enzym. Inhib. Med. Chem. 36 (1) (2021) 561–580, https://doi.org/10.1080/14756366.2021.1882453.
[56] D. Moi, A. Nocentini, A. Deplano, G. Balboni, C.T. Supuran, V. Onnis, Structure-activity relationship with pyrazoline-based aromatic sulfamates as carbonic anhydrase isoforms I, II, IX and XII inhibitors: synthesis and biological evaluation, Eur. J. Med. Chem. 182 (2019) 111638, https://doi.org/10.1016/j.ejmech.2019.111638.
[57] J.n. Ivanova, A. Nocentini, K. Tārs, J.n. Leitāns, E. Dvinskis, A. Kazaks, I. Domračeva, C.T. Supuran, R. Žalubovskis, Atropo/tropo flexibility: a tool for design and synthesis of self-adaptable inhibitors of carbonic anhydrases and their antiproliferative effect, J. Med. Chem. 66 (8) (2023) 5703–5718, https://doi.org/10.1021/acs.jmedchem.3c00007.
[58] M. Abdoli, V. De Luca, C. Capasso, C.T. Supuran, R. Žalubovskis, Inhibition studies on carbonic anhydrase isoforms I, II, IX, and XII with a series of sulfaguanidines, ChemMedChem 18 (6) (2023) e202200658, https://doi.org/10.1002/cmdc.202200658.
[59] M.S. Popoviciu, L. Paduraru, R.M. Nutas, A.M. Ujoc, G. Yahya, K. Metwally, S. Cavalu, Diabetes mellitus secondary to endocrine diseases: an update of diagnostic and treatment particularities, Int. J. Mol. Sci. 24 (16) (2023) 12676, https://doi.org/10.3390/ijms241612676.
[60] C.I. Chukwuma, R. Mopuri, S. Nagiah, A.A. Chuturgoon, M.S. Islam, Erythritol reduces small intestinal glucose absorption, increases muscle glucose uptake, improves glucose metabolic enzymes activities and increases expression of Glut-4 and IRS-1 in type 2 diabetic rats, Eur. J. Nutr. 57 (7) (2018) 2431–2444, https://doi.org/10.1007/s00394-017-1516-x.
[61] C.N. Suire, M.D. Hade, Extracellular vesicles in type 1 diabetes: a versatile tool, Bioengineering 9 (3) (2022) 105, https://doi.org/10.3390/bioengineering9030105.
[62] H.A. El-Nashar, N.M. Mostafa, M. El-Shazly, O.A. Eldahshan, The role of plant-derived compounds in managing diabetes mellitus: a review of literature from 2014 to 2019, Curr. Med. Chem. 28 (23) (2021) 4694–4730, https://doi.org/10.2174/0929867328999201123194510.
[63] N. Lolak, S. Akocak, M. Durgun, H.E. Duran, A. Necip, C. Türkeş, M. Işık, Ş. Beydemir, Novel bis-ureido-substituted sulfaguanidines and sulfisoxazoles as carbonic anhydrase and acetylcholinesterase inhibitors, Mol. Divers. 27 (4) (2023) 1735–1749, https://doi.org/10.1007/s11030-022-10527-0.
[64] J.A. Verpoorte, S. Mehta, J.T. Edsall, Esterase activities of human carbonic anhydrases B and C, J. Biol. Chem. 242 (18) (1967) 4221–4229, https://doi.org/10.1016/S0021-9258(18)95800-X.
[65] Y. Tao, Y. Zhang, Y. Cheng, Y. Wang, Rapid screening and identification of α-glucosidase inhibitors from mulberry leaves using enzyme-immobilized magnetic beads coupled with HPLC/MS and NMR, Biomed. Chromatogr. 27 (2) (2013) 148–155, https://doi.org/10.1002/bmc.2761.
[66] Z. Xiao, R. Storms, A. Tsang, A quantitative starch? Iodine method for measuring alpha-amylase and glucoamylase activities, Anal. Biochem. 351 (1) (2006) 146–148, https://doi.org/10.1016/j.ab.2006.01.036.
[67] H. Lineweaver, D. Burk, The determination of enzyme dissociation constants, J. Am. Chem. Soc. 56 (3) (1934) 658–666, https://doi.org/10.1021/ja01318a036.
[68] M.S. Blois, Antioxidant determinations by the use of a stable free radical, Nature 181 (4617) (1958) 1199–1200, https://doi.org/10.1038/1811199a0.
[69] R. Re, N. Pellegrini, A. Proteggente, A. Pannala, M. Yang, C. Rice-Evans, Antioxidant activity applying an improved ABTS radical cation decolorization assay, Free Radical Biol. Med. 26 (9) (1999) 1231–1237, https://doi.org/10.1016/S0891-5849(98)00315-3.
[70] S. Chakravarty, K.K. Kannan, Drug-protein interactions: refined structures of three sulfonamide drug complexes of human carbonic anhydrase I enzyme, J. Mol. Biol. 243 (2) (1994) 298–309, https://doi.org/10.1006/jmbi.1994.1655.
[71] K.H. Sippel, A.H. Robbins, J. Domsic, C. Genis, M. Agbandje-McKenna, R. McKenna, High-resolution structure of human carbonic anhydrase II complexed with acetazolamide reveals insights into inhibitor drug design, Acta Crystallogr. F 65 (10) (2009) 992–995, https://doi.org/10.1107/S1744309109036665.
[72] V. Roig-Zamboni, B. Cobucci-Ponzano, R. Iacono, M.C. Ferrara, S. Germany, Y. Bourne, G. Parenti, M. Moracci, G. Sulzenbacher, Structure of human lysosomal acid α-glucosidase–a guide for the treatment of Pompe disease, Nat. Commun. 8 (1) (2017) 1111, https://doi.org/10.1038/s41467-017-01263-3.
[73] Schrödinger Release 2024-1: Protein Preparation Wizard, Schrödinger, LLC, New York, NY, 2024.
[74] A. Buza, C. Türkeş, M. Arslan, Y. Demir, B. Dincer, A.R. Nixha, Ş. Beydemir, Discovery of novel benzensulfonamides incorporating 1,2,3,-triazole scaffold as carbonic anhydrase I, II, IX, and XII inhibitors, Int. J. Biol. Macromol. 239 (2023) 124232, https://doi.org/10.1016/j.ijbiomac.2023.124232.
[75] Schrödinger Release 2024-1, LigPrep, Schrödinger, LLC, New York, NY, 2024.
[76] C. Türkeş, Y. Demir, Ş. Beydemir, Infection medications: assessment in-vitro glutathione S-transferase inhibition and molecular docking study, ChemistrySelect 6 (43) (2021) 11915–11924, https://doi.org/10.1002/slct.202103197.
[77] Schrödinger Release 2024-1, Epik, Schrödinger, LLC, New York, NY, 2024.
[78] C. Kakakhan, C. Türkeş, Ö. Güleç, Y. Demir, M. Arslan, G. Özkemahlı, Ş. Beydemir, Exploration of 1,2,3-triazole linked benzensulfonamide derivatives as isoform selective inhibitors of human carbonic anhydrase, Bioorg. Med. Chem. 77 (2023) 117111, https://doi.org/10.1016/j.bmc.2022.117111.
[79] Schrödinger Release 2024-1: SiteMap, Schrödinger, LLC, New York, NY, 2024.
[80] Schrödinger Release 2024-1: Receptor Grid Generation, Schrödinger, LLC, New York, NY, 2024.
[81] Schrödinger Release 2024-1, Maestro, Schrödinger, LLC, New York, NY, 2024.
[82] C. Türkeş, Carbonic anhydrase inhibition by antiviral drugs in vitro and in silico, J. Mol. Recogn. 36 (12) (2023) e3063, https://doi.org/10.1002/jmr.3063.
[83] Schrödinger Release 2024-1: Glide, Schrödinger, LLC, New York, NY, 2024.
[84] Ö. Güleç, C. Türkeş, M. Arslan, Y. Demir, B. Dincer, A. Ece, Ö.İ. Küfrevioğlu, Ş. Beydemir, Novel spiroindoline derivatives targeting aldose reductase against diabetic complications: Bioactivity, cytotoxicity, and molecular modeling studies, Bioorg. Chem. 145 (2024) 107221, https://doi.org/10.1016/j.bioorg.2024.107221.
[85] S. Dawbaa, C. Türkeş, D. Nuha, Y. Demir, A.E. Evren, L. Yurttaş, Ş. Beydemir, New N-(1,3,4-thiadiazole-2-yl)acetamide derivatives as human carbonic anhydrase I and II and acetylcholinesterase inhibitors, J. Biomol. Struct. Dyn. (2024) 1–19, https://doi.org/10.1080/07391102.2024.2331085.
[86] Schrödinger Release 2024-1: Prime, Schrödinger, LLC, New York, NY, 2024.
[87] H. Muğlu, H. Yakan, M. Erdoğan, F. Topal, M. Topal, C. Türkeş, Ş. Beydemir, Novel asymmetric biscarbothioamides as Alzheimer's disease associated cholinesterase inhibitors: synthesis, biological activity, and molecular docking studies, New J. Chem. 48 (2024) 10979–10989, https://doi.org/10.1039/d4nj01462f.
[88] C. Türkeş, S. Akocak, M. Işık, N. Lolak, P. Taslimi, M. Durgun, İ. Gülçin, Y. Budak, Ş. Beydemir, Novel inhibitors with sulfamethazine backbone: synthesis and biological study of multi-target cholinesterases and α-glucosidase inhibitors, J. Biomol. Struct. Dyn. 40 (19) (2022) 8752–8764, https://doi.org/10.1080/07391102.2021.1916599.
[89] Ö. Güleç, C. Türkeş, M. Arslan, Y. Demir, B. Dincer, A. Ece, Ş. Beydemir, Novel beta-lactam substituted benzenesulfonamides: in vitro enzyme inhibition, cytotoxic activity, and in silico interactions, J. Biomol. Struct. Dyn. 42 (12) (2024) 6359–6377, https://doi.org/10.1080/07391102.2023.2240889.
[90] Schrödinger Release 2024-1: QikProp, Schrödinger, LLC, New York, NY, 2024.
[91] A. Daina, O. Michielin, V. Zoete, SwissADME: a free web tool to evaluate pharmacokinetics, drug-likeness and medicinal chemistry friendliness of small molecules, Sci. Rep. 7 (1) (2017) 42717, https://doi.org/10.1038/srep42717.
[92] C.A. Lipinski, F. Lombardo, B.W. Dominy, P.J. Feeney, Experimental and computational approaches to estimate solubility and permeability in drug discovery and development settings, Adv. Drug Deliv. Rev. 23 (1) (1997) 3–25, https://doi.org/10.1016/S0169-409X(96)00423-1.
[93] E.M. Duffy, W.L. Jorgensen, Prediction of properties from simulations: free energies of solvation in hexadecane, octanol, and water, J. Am. Chem. Soc. 122 (12) (2000) 2878–2888, https://doi.org/10.1021/ja993663t.